

Examensarbete
TVVR 07/5019

Soil Water Modelling In Arid/Semiarid Regions of Northern China Using Land Information System (LIS)

A Minor Field Study in Shiyang River Basin

Sara Dahlgren
Björn Possling



Water Resources Engineering
Department of Building and Environmental Technology
Lund University

Soil Water Modelling In Arid/Semiarid Regions of Northern China Using Land Information System (LIS)

A Minor Field Study in Shiyang River Basin

Sara Dahlgren
Björn Possling



LUNDS TEKNISKA HÖGSKOLA

Lunds universitet

Lund University

Faculty of Engineering, LTH

Departments of Earth and Water Engineering

This study has been carried out within the framework of the Minor Field Studies (MFS) Scholarship Programme, which is funded by the Swedish International Development Cooperation Agency, Sida.

The MFS Scholarship Programme offers Swedish university students an opportunity to carry out two months' field work in a developing country resulting in a graduation thesis work, a Master's dissertation or a similar in-depth study. These studies are primarily conducted within subject areas that are important from an international development perspective and in a country supported by Swedish international development assistance.

The main purpose of the MFS Programme is to enhance Swedish university students' knowledge and understanding of developing countries and their problems. An MFS should provide the student with initial experience of conditions in such a country. A further purpose is to widen the human resource base for recruitment into international co-operation. Further information can be reached at the following internet address: <http://www.tg.lth.se>, click at "MFS-stipendier".

The responsibility for the accuracy of the information presented in this MFS report rests entirely with the authors and their supervisors.

Gerhard Barmen
Local MFS Programme Officer

Abstract

At present China suffers from severe desertification or land degradation. About 27% of the total territory was exposed in 2004, mainly the northern provinces. Consequences of desertification, such as floods or sandstorms, require huge effort and financial assets. Soil moisture understanding plays a key role in combating desertification and is necessary in order to implement a sustainable water management.

Land Surface Models (LSMs) are one approach to survey and quantify soil moisture. A LSM calculates the surface state from physical conceptual equations based on satellite derived input. Land Information System (LIS) is a framework for global modelling with LSMs. LIS has a high spatial and temporal resolution and the ability to simulate soil moisture and other water related parameters in a near real time manner. There are several kinds of LSMs but currently only two are implemented in the Land Information System (LIS); namely Noah and CLM. LIS is designed to be flexible in terms of atmospheric input data and can use one of many sources.

The main aim with this thesis is to investigate LIS as a tool in water management in arid /semiarid regions. The two LSMs within LIS were simulated and compared over several investigation points widely distributed over Shiyang river basin, northern China. This was done in order to find possibilities and limitations with LIS and potential differences between the LSM interpretations in this setting.

The study consists of two parts. Part one is a field study in an arid area in Gansu, China, during September 2006. Part two is computer simulations using the model framework LIS and its different LSMs with altered atmospheric input over the Shiyang river basin. The aims of the simulations were first to find a good configuration for modelling the area and then to investigate differences in LSM interpretation. Noah and CLM were compared in a four year simulation starting January 1st 2000 and in a created rain scenario to observe infiltration patterns.

The field measurements showed average soil moisture of 6.6% in the top ten cm and 11.8% in the 10-30 cm layer during September. The simulations showed the forcing option GDAS to give best performance of precipitation interpolation accuracy. A slightly higher initial soil moisture value than the regional average could give a quicker spin up time.

The four-year simulation indicated differences between Noah and CLM in spin up time and soil moisture patterns. The constructed rain event revealed Noah to percolate more rapidly and to a greater extent than CLM. CLM lost water and the reason could be traced to surface and subsurface runoff, rather than evaporation.

LIS is still in a developing state and updates are released regularly. Necessary input data was unavailable during the research, due to server problems. Further investigation of soil moisture fluctuation is therefore needed to ensure if any LSM is more preferable in this region. One advantage using LIS is however the possibility to run simulations with different set up and consider all results.

Keywords

Land Surface Modelling, Land Information Systems, Soil Moisture, Noah, CLM

Sammanfattning

Ökenspridning är ett allvarligt problem i Kina. Cirka 27 % av Kinas totala yta uppskattades vara påverkad av ökenspridning 2004. Konsekvenserna från detta, såsom översvämningar och sandstormar kostar Kina stora resurser i form av pengar och arbetskraft. En större förståelse av fluktuationerna i de översta lagrens markvattenhalt är viktig i processen för att på rätt sätt starta projekt för att hindra ökenspridningen.

Land Surface Models (LSM) är ett försök att studera mängden markvatten. En LSM beräknar markytans tillstånd med hjälp av ekvationer och indata hämtad och tolkad från satellitbilder. Land Information System (LIS) är ett ramverk för global modellering med LSM:er. LIS har hög rums- och tidsupplösning och erbjuder möjligheter att modellera vatten- och energiflöden i nära realtid. Det finns en mängd olika LSM:er, LIS har för närvarande implementerat användandet av två, Noah och CLM. LIS har möjlighet att använda många olika källor för indata.

Huvuduppgiften med denna uppsats är att undersöka LIS som ett redskap vid planerandet av vatten resurser för ökenspridningsbekämpning i arida/semiarida miljöer. Noah och CLM har jämförts i flera punkter utspridda i avrinningsområdet Shiyang i norra Kina. Detta var gjort med avsikten att finna styrkor och svagheter med LIS och skillnader mellan Noah och CLM i en miljö som denna.

Studien bestod av två delar. Del ett var en fältstudie i ett aritt område i Gansu, Kina, utförd i september 2006. Del två bestod av datorsimuleringar i LIS. Simuleringarna gjordes för att finna bra inställningar för att köra LIS i denna miljö, samt att undersöka resultaten från en fyraårskörning, med start januari 2000 samt en simulering av ett regnscenario för att undersöka infiltrationsmönster.

Enligt fältstudien var halten markvatten i september i genomsnitt 6.6 % i de översta 10 cm av markprofilen och 11.8 % i skiktet 10-30 cm. Simuleringar visade att GDAS som källa för regndata gav bäst resultat, samt att initialvärdet av markfuktighet kan sättas lite högre än väntat för att få systemet att ställa in sig snabbare.

Fyraårssimuleringarna visade på skillnader mellan Noah och CLM vad gäller tiden det tar att stabilisera systemet, samt fluktuationer i markvattenhalten. Det konstruerade regnscenariot visade att Noah låter vatten infiltrera djupare än CLM. CLM förlorade stora mängder vatten genom avrinning på och under markytan.

LIS är fortfarande under utveckling och nya versioner av programmet släpps med jämna mellanrum. Under studien var stora delar av indata otillgängliga på grund av problem med servrar hos NASA. Fortsatta studier av markvattenfluktuationer är nödvändiga för att kunna avgöra vilken LSM som är att föredra i området. En av LIS största styrkor är dock möjligheten att enkelt köra modellen flera gånger med olika inställningar och ta alla resultat i beaktning.

Acknowledgement

This diploma work was made possible thanks to the Minor Field Study (MFS) program, financed by the Swedish International Development Cooperation Agency (SIDA). SIDA is a government agency under the Swedish Ministry for Foreign Affairs, which founded the MFS program with the intention of widening the knowledge about developing countries and encourage intercollaboration.

We would like to express our gratitude to our supervisor Linus Zhang at the Department of Water Resources Engineering at the faculty of Engineering, Lund University (LTH), whose support and guidance facilitated both our investigation and our acquaintance with China.

We would also like to express our appreciation to our supervisor in China, Prof. Zhao Yuan Zhong and the staff at Gansu Irrigation and Training Center (GS-CIET), Lanzhou. You were all very friendly and supportive. A special thanks to Xie Xieling for efficient translation and friendship during our stay in China.

The field station where our experiments were conducted was governed by Prof. Shaozhong Kang, China Agriculture University. Our work at the station would not have been possible without the help from professor Kang. We would also like to thank all our friends from the Beijing University who were also staying in the field station. Thanks for making our stay there so pleasant.

And finally we would like to give a special thank to Mr. Yong Zheng at GS-CIET for his warm welcoming to China and around the clock aid. You took care of all the needs we could possibly have, regarding everything from technical guidance to local bars. Thanks a lot!

Table of Contents

1 Background	1
1.1 Problem Statement	1
1.1.1 Land Degradation in China	1
1.1.2 Desertification - Related Research	2
1.2 Study Area	3
1.2.1 The Gansu province and Shiyang River Basin	3
1.2.2 Hydrological Description of Shiyang River Basin	4
1.2.3 Water Resources and Utilization within Shiyang	4
1.2.4 Desertification- Impact on the Eco-Environment in Shiyang	5
1.3 Thesis Outline	6
1.3.1 Objectives	7
2 Field Study	8
2.1 The Wuwei Field Station	8
2.2 Soil Moisture Measurements at the Field	9
2.2.1 Mapping	9
2.2.2 Soil Moisture Measurements	11
2.2.2.1 TDR	12
2.2.2.2 Soil Sampling with PVC tube	12
2.2.2.3 Soil Sampling with Drill	13
2.2.3 Density Measurements	14
2.2.4 Data Post Processing	14
2.2.5 Meteorological Recordings	15
2.2.6 Sources of Error	15
2.2.6.1 Scale	15
2.2.6.2 TDR	15
2.2.6.3 PVC method	16
2.2.6.4 Drill Method	16
2.2.6.5 GPS	16
2.2.6.6 Metrological Recordings	16
2.3 Results and Discussion	16
3 Environmental Modelling	18
4 LIS Description	19
4.1 Land Surface Models (LSM)	19
4.1.1 Noah	20
4.1.2 CLM	21
4.3 LIS Input	21
4.3.1 Atmospheric Forcings	21
4.3.1.1 Base Forcing	22
4.3.1.2 Supplementary Forcings	22
4.3.2 Parameter Data	23
4.4 LIS Requirements and Software	23
4.4.1 Lunarc	23
4.4.2 GrADS	24
5 Statistical Approach	25
5.1 Mean Absolute Error, MAE	25
5.2 Total Error	25

5.3 Sample Correlation Coefficient, r	25
6 Simulated Area	26
6.1 Precipitation Data	26
6.1.1 Precipitation Validation Data; Hydrological Bureau of Gansu.....	26
6.1.2 Precipitation Validation Data; China West	26
6.2 Shiyang Soil Moist Survey	26
7 LIS Methodology	28
7.1 Configuration and Set Up.....	28
7.1.1 Forcing Precipitation Validation and LIS Interpolation Evaluation.....	28
7.1.1.1 LIS Precipitation Interpretation.....	28
7.1.1.2 Data Retrieval from Forcings	28
7.1.1.3 Data Comparing	28
7.1.2 Spin Up Test.....	29
7.2 Soil Moisture	29
7.2.1 Comparison of Noah and CLM Over a Four Year LIS Run	30
7.2.2 Modelling Constructed Rain	31
8 Results and Discussion.....	32
8.1 Configuration and Set Up.....	32
8.1.1 Forcing Precipitation Validation and LIS Interpolation Evaluation.....	32
8.1.2 Spin Up Test.....	33
8.2 Soil Moisture Simulation.....	34
8.2.1 Comparison of Noah and CLM Over a Four Year LIS run.....	34
8.2.2 Modelling Constructed Rain	37
9 Conclusions	41
References	42
Appendices	46
Appendix A - Abbreviations	46
Appendix B - Precipitation Data	47
Appendix C - Soil Moist Measurements, Wuwei September 2006	49
Appendix D – File Examples	51
Appendix E - Comparison of Noah and CLM over a Four Year LIS Run.....	58

1 Background

1.1 Problem Statement

1.1.1 Land Degradation in China

The problem and cause of land degradation or desertification has been in focus in China since the 1970's. The primary cause has been identified as anthropogenic impact, although northern China also experienced a climatic change towards increasing aridity during 1960s-1990s. The rapidly increasing population lead to intensified food demand which required agricultural expansion, with consequences of deforestation, overgrazing and, in extension, land degradation.¹ At present China suffers from severe land degradation. In 2004 an area of 2,636,200 km² or 27% of the total Chinese territory was exposed to desertification or sandification. These areas are widely distributed over 18 provinces, located mainly in the northern part of China.² Desertification related damage caused by floods or sandstorms require huge efforts for the country. Sandstorms alone cost around 54 billion Yuan/year (6.5 billion US\$/year).³

Governmental concerns contributed to several national land conservation campaigns where the overall preventive strategy was to minimize soil erosion by recreating or maintaining natural habitats. The *Three-north forest shelter belt project* was launched in 1978. The intention was to revegetate 28 million hectares of desert and restore 95 million hectares of forest in the exposed areas of northern China. This large-scale project aimed at improving and protecting environment with local agriculture and industry maintained at its present level. Parts of the project were successful although the approach mainly showed undesirable results. Planted vegetation showed a low survival percentage, which in some areas even escalated desertification.⁴

The main reason for the *Natural forest resources protection project* was to reduce flooding along the Yangtze and Yellow river. The preserving measures prohibited logging in 1998, which in turn resulted in substantial unemployment in forestry. In 1999 another preventative program was launched due to the increasing frequency of sandstorms and floods.⁵

The *grain for green project* took place in Sichuan, Shaanxi and Gansu provinces where farmers were obligated to replace their crop fields with trees and grass during a time period depending on local conditions. For this they got compensation based on the size of their changed farmland. This turned out somewhat successfully and is now implemented in larger scale involving the upper reaches of Yangtze and the middle and upper reaches of the Yellow river.⁶

Failure in combating desertification could be traced to three problem areas: non-scientific decision making, neglect of social aspects and a lack of well organized monitoring systems.

¹ Chen, Y., and H. Tang, 2005

² CCICCD, 2006

³ Yang, H., 2004

⁴ Ibid.

⁵ Ibid.

⁶ Ibid.

The sensitivity of the ecosystems dominating the arid/semiarid regions of northern China has been well known and documented for quite some time. Scientists agree that preventing measures need to be done in small scale considering local conditions. This however, has been overlooked in the governmental strategy. National land management has almost exclusively concerned planting trees and grass, regardless of local requirements and with varying results. The national strategy has also neglected the needs of the local inhabitants. The rural areas are distinguished by poor living conditions where the locals are depending on pasture and agriculture. Restrictions for grazing and land use will therefore directly affect their livelihood. Without a drastic improvement of living standards the long term goal of land reclamation will never be achieved.⁷ Finally, the lack of a well organized monitoring system has complicated the land reclamation process. Long term records of land degradation impacts and extent are necessary for choosing an effective strategy and for evaluating precautions.⁸ Preventing measures has slowed down the desertification process, the situation is however still crucial and in desperate need of further attention to ensure Chinas continued development.

1.1.2 Desertification - Related Research

Desertification related research has recently been devoted to monitoring, water resource management and to widening the understanding of biosphere dynamics. Linking the different areas of expertise is the general understanding of soil moisture, its spatial and temporal behaviour.

Monitoring research has almost exclusively been dedicated to different remote sensing techniques. Since land degradation has been associated with a decrease in biologic productivity,⁹ a common measurement for surveys in China has been the normalized difference vegetation index (NDVI).¹⁰ NDVI is based on the difference in reflectance between the near infrared and the red wavelengths and is highly correlated to the Leaf Area Index (LAI), which is the one sided green leaf area to the total surface area. By using this technique natural oases could be monitored and compared over time. This was done over the Hexi region during 1995 through 2003 showing a 5 % decrease in natural oasis.¹¹ There is a technical weakness in the NDVI determination when the soil background tends to disturb the satellite observations influencing the perception of the land cover.¹² Research is still focused on improvements to take these disturbances into account.

The distribution and the possibility to quantify assets of surface water have been investigated at a catchment scale using MIKE BASIN. This model has been implemented in Shule basin, northwest China, as an attempt to estimate water resources. With limited data such as averages of precipitation and evaporation, MIKE BASIN could be used to get a rough water balance, realizing supplies, which could be useful when planning irrigation schemes and withdrawal rates.¹³

⁷ Chen, Y., and H. Tang, 2005

⁸ Chen, Y., 2005

⁹ Prince, S.D, 2002

¹⁰ Liu, A.X. et al., 2003

¹¹ Liao, L., et al., 2005

¹² Runnström, M., 2003

¹³ Oelert, A., and D. Rosbjerg, 2006

As an attempt to allocate water resources efficiently several irrigation techniques have been implemented and investigated throughout China. Using sprinkling techniques instead of flood irrigation could save about 30-50% water.¹⁴ Regular sprinkling is however not appropriate in dry and windy conditions and within arid regions another method known as microirrigation has indicated promising results. By using dripping irrigation around 90% efficiency could be achieved.¹⁵ Nonetheless, this method is recognized to be difficult to operate and is also quite pricey. An alternative to irrigation schemes is to alter the land use. Transforming crop fields into grasslands could increase precipitation efficiency with 14-29%.¹⁶

The intension of the global soil wetness project (GSWP) was to monitor soil moisture with remote sensing techniques. Previous attempts of soil water surveys had faced difficulties. For instance, microwave techniques only worked over sparsely vegetated areas, and gamma radiation methods could only estimate water content to a depth of 20 centimetres. For a more general and deeper survey, soil moisture had to be modelled. For this purpose land surface models calculating the land surface condition, and soil water content, were developed. GSWP was carried out in the 1990's as a global effort to develop and investigate different land surface schemes and establish a framework for soil water modelling.¹⁷ The land surface models used today, such as CLM and Noah, are based on these schemes.

1.2 Study Area

1.2.1 The Gansu province and Shiyang River Basin

Gansu province is located in the northwest part of China bordering to Mongolia in the north, see Figure 1. The surrounding Chinese provinces in a clockwise order are; Inner Mongolia to the northeast, Ningxia, Shaanxi in the southeast, Sichuan in the south, Qinghai to the west and Xinjiang in the northwest. Gansu province has an area of 454 000 km² and houses 26.3 million habitants. 1.4 million people are living in the province capital, Lanzhou.



Figure 1. China with Gansu province.

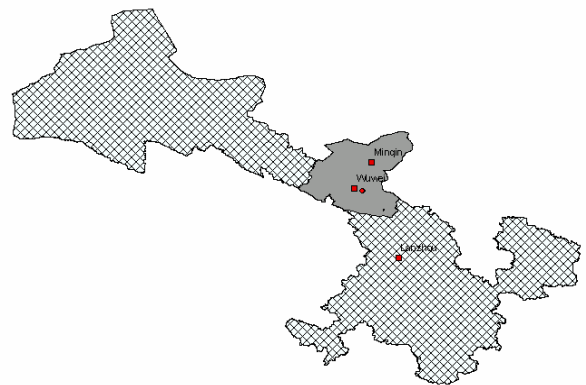


Figure 2. Gansu province with Shiyang river basin shaded.

¹⁴ Yang, Y. et al., 2002

¹⁵ Ibid.

¹⁶ Zhao, X., 2005

¹⁷ Dirmeyer, P.A., et al., 1999

Situated in the Hexi corridor, within Gansu province, is the Shiyang river basin represented as the shaded part in Figure 2. The basin has an area of 41 600 km² with a geographic stretch between longitude 101.68° – 104.27° E and latitude 36.48° – 39.45° N.¹⁸ Parting the basin into a northern and a southern half is the mountain chain from Longshoushan to Hongyashan. Shiyang river basin reaches from the Qilian Mountains in the south to the Tengger and Badanjilin deserts in the north. Shiyang includes part of Zhangye Municipality large areas of Wuwei Municipality (Minqin County included) and Jinchang Municipality.¹⁹

1.2.2 Hydrological Description of Shiyang River Basin

The catchment could be divided into three distinct zones due to differences in climate, hydrology and ecology. Uniting the basin is the inland river Shiyang and its eight tributaries. The tributary rivers from west to east are: Xida, Dongda, Xiyin, Jinta, Zamu, Huangyang, Gulang and Dajin river.

The Shiyang river starts in the Qilian Mountains, zone one, where it is fed by precipitation and snow melt. Here the elevation is about 2000-5000 m.a.s.l and the precipitation and potential evaporation is 300-600 mm and 700-1200 mm respectively. The river continues through zone two, the corridor plain, which is characterized by a cooler and more arid climate. Here the annual precipitation and potential evaporation is 150-300 mm and 1200-2000 mm respectively. The corridor plain has an altitude of about 1500-2000 m.a.s.l The northern part of Shiyang, zone three, has a lower elevation of 1300-1500 m.a.s.l. The climate in this region is warmer and more arid. The annual precipitation is less than 150 mm and the potential evaporation between 2000-2600 mm.²⁰

1.2.3 Water Resources and Utilization within Shiyang

Between the years 1950 through 2000 Shiyang doubled its population to 2.23 million people. The majority of which inhabited the rural areas. The rapid population expansion resulted in a considerable change of natural land into cultivated, affecting the water utilization. During this period irrigated areas increased with 139 %. The industrial water usage is negligible compared to the proportion used for irrigation. In year 2000 Wuwei and Jinchang municipality used $28.39 \cdot 10^8 \text{ m}^3$ water of which 90.3% was used for irrigation of crop and forest. Even if the percentage used for irrigation has decreased slightly since 1980, the total water consumption has increased. The growing demand of water declined surface water supplies and increased ground water abstraction. The consequences were more significant downstreams and Minqin County faced a depletion of ground water resources and a spreading desertification.²¹

To address the water shortage in Minqin, water was imported from the Yellow river via the Jindian-Minqin canal. The canal construction was finished 2001 with a capacity to transport 61 million m³ water each year. 46 million m³ were transferred in 2001 and nothing in 2002 due to too high expenses for the locals. Since Minqin County had no monetary assets to fund the importation the county requested upstream counties or governmental contribution as

¹⁸ Kang, S., et al., 2004

¹⁹ Hu, W., 2005

²⁰ Kang, S., et al., 2004

²¹ GPDPC & GDPWR, 2003

compensation. This raised the issue of claiming responsibility with suggestions of economic compensation or penalty fees as a solution.²²

All rivers within Shiyang, except Zamu river, are controlled by reservoirs and dams. When regulating surface water in dams and reservoirs under arid conditions evaporation losses become considerable. Hongyashan reservoir loses around 23 million m³ water each year. This represents 24% of its total capacity.²³ With 23 dams within the basin the total evaporation loss is estimated to 108 million m³ each year, which exceeds the discharge from Shiyang River to the Minqin area. Further more the dams are known to have a minor effect in regulating flooding and reusing natural aquifers might be considered as a more efficient way to preserve water supplies.²⁴

1.2.4 Desertification- Impact on the Eco-Environment in Shiyang

During the 1950's several perennial herbaceous plants were introduced in the vicinity of Minqin oasis. The intension was to protect the oasis from degradation with its capacity to work as sand-fixers and windbreakers. Since then the protective vegetation as well as the oasis have suffered from sever deterioration due to the declining water table and soil salinization. The degradation could be emphasized with the decrease of vegetation coverage, which was 44.8 % in the 1950's and decreased to less than 15% in 2001.²⁵ During the same time period the oasis area decreased by 18% and is today one of the driest places nationwide facing further degradation.²⁶

Research found stable ground water levels to be of equal importance as supplied irrigation in plant survival.²⁷ The critical ground water depth is known to be both vegetation- and region specific. The most efficient ground water depth should be deep enough to avoid evaporation and saline development in the soil, but shallow enough to be accessible to the existing vegetation. Dominant vegetation in the area are xerophytic shrubs tolerant to the dry circumstances such as *Artemisia Ordosica* and *Nitrana Tangatonium*.²⁸ Most oasis vegetation require a ground water level between 3.5-4 meters, few plants survive levels deeper than 10 meters.²⁹ Nevertheless, soils with the water table within 2 meters are known to be more saline,³⁰ so a preferable ground water depth should be around 2-4 meters to avoid further deterioration of the region.

Today Shiyang is facing the most serious water shortage in the Hexi corridor, due to its expansion of agricultural and industrial activity. The ground water table is lowered by an average of 0.4-0.8 m/year and combined with a loss of vegetation makes the region in threat of further desertification.³¹

²² Zhu, F., 2004.

²³ GPDPC & GPDWR, 2003

²⁴ Hu, W., 2005

²⁵ Zhang, Y., 2001

²⁶ Hu, W., 2005

²⁷ Si, J. et al., 2004

²⁸ Hu, W., 2005

²⁹ Guo, Z. and Liu, H. 2005

³⁰ Ellis, S., and Mellor, A., 1995

³¹ Kang, S., et al., 2004

1.3 Thesis Outline

The purpose of this case study was to investigate the Land Information System (LIS) under arid/semiarid conditions, based on field studies of some key hydrological parameters and a high resolution numerical modelling system. Two LSMs were studied further: Noah and CLM. The intention was to realize the possibilities and limitations of LIS in land surface modelling and its potential as a tool in water resource management.

LIS has the potential of being the optimal tool in water resource management. With its high spatial and temporal resolution it has the ability to simulate soil moisture and other water related parameters in a near real time manner. Taking in consideration the local differences of elevation, soil type and existing canopy, LIS has the ability to calculate the surface's condition and the possibility of doing so with a global coverage.³²

LIS is a framework for land surface modelling, developed by the Goddard Space Flight Center (GSFC) at NASA. A simplified scheme of LIS can be found in Figure 3. The LIS driver interprets and interpolates atmospheric input data (forcing data) with global coverage into its own high resolution grid. Apart from the atmospheric forcings, surface parameters and an initial soil state is required. The one-dimensional Land Surface Model (LSM) is then to calculate the surface state variables for each grid cell and time step. The LIS driver is then coordinating the information from the LSM into a data set for the time step and writes output data with spatial coverage accessible for the user.³³

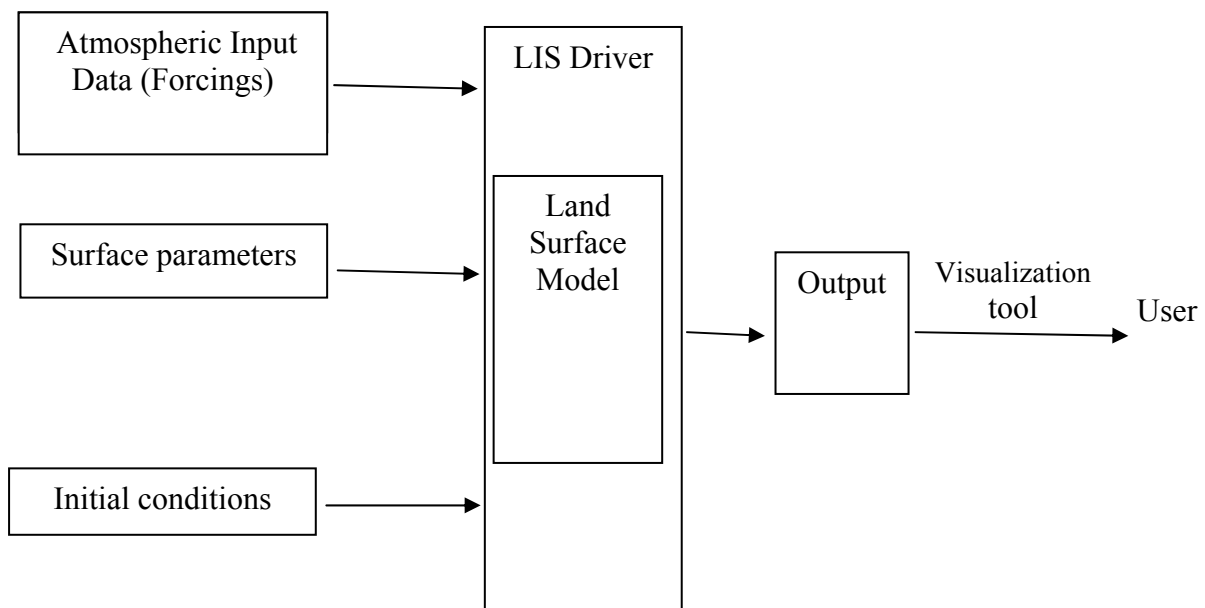


Figure 3. Schematic description of LIS.

The project was part of a research program at the Gansu Irrigation and Training Center (GS-CIET), Lanzhou, China. The collaboration between LTH and GS-CIET provided the opportunity to investigate LIS under these conditions.

³² NASA/GSFC, 2007

³³ NASA/GSFC, 2007

For this master thesis Shiyang river basin was chosen to represent arid/semiarid conditions. The investigated parameters were soil moisture and precipitation where computer simulated values were compared with actual measurements. The investigation was performed in two parts. Part one was a field study supervised by Zhao Yuan Zhong at GS-CIET and performed during September 2006 in rural China. Part two was computer simulations using LIS at the Department of Water Resources Engineering at the Faculty of Engineering (LTH), Lund University with the guidance of associate professor Linus Zhang.

During a four weeks field study soil moisture measurements were gathered. At the same time the China Agriculture University (CAU) collected meteorological data, which is also included in the investigation. The field work was supervised by Mr. Yuan Zhong Zhao and Mr. Yong Zheng at the Gansu Irrigation and Training Center.

1.3.1 Objectives

This thesis aims at investigating the possibilities and limitations of Land Information System as a tool for desertification alleviation planning in the arid to semiarid conditions of rural China. The following aspects of LIS modelling have been studied:

- What is the best LIS configure in terms of forcing data and initial states?
- Which LSM gives the most reliable soil moisture simulations?

A field study was conducted to obtain soil moisture values in an arid/semiarid region to compare with LIS modelling results.

2 Field Study

2.1 The Wuwei Field Station

Located in the Shiyang river basin, southeast from Wuwei is the Shiyanghe Experimental Station for Water Saving in Agriculture and Ecology. The station is situated in the Wuwei oasis see, Figure 4 below. The station is located in the semiarid climate zone and under the surveillance of China Agriculture University. It is governmentally founded with the intension of research of water related issues.

The area houses a recreational park for tourists as well as several desertification alleviation projects. At present many agriculture-related experiments are performed, such as evaluation of saline tolerance and water consumption of various natural desert plants. There are also experiments on water saving methods such as new irrigation techniques and the possibility of reducing the amount of irrigation water without losing crop yield. Other experiments focus on infiltration and evapotranspiration in order to gain hydrologic knowledge about the area. Figure 5 shows some pictures from the station and some ongoing projects.

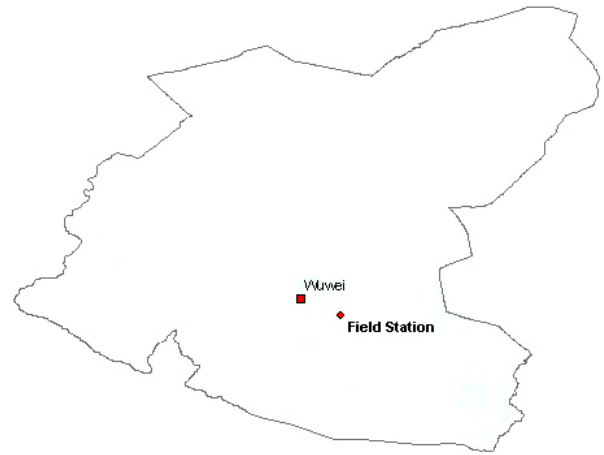


Figure 4. The location of the field station, southeast of Wuwei.



Figure 5. The field station and experiments conducted there; infiltration, saline tolerance of desert vegetation and evaporation estimations.

2.2 Soil Moisture Measurements at the Field

During the first days of September thirteen points just outside Desert Park were chosen for investigation of soil moisture. The site was chosen to represent a semiarid environment as much as possible. Sand dunes were dominating the area giving it a hilly character. The crests were generally very dry while some troughs were used to grow corn or other crops. The fields were said not to be irrigated but some dry irrigation ditches were found in the area. The soil of many of the fields was covered with a thin plastic film. This is a commonly used water saving technique to lower the evaporation. The vegetation on the sandy area was sparse and consisted mostly of small shrubs and ground level plants. See Figure 11-14. Each point was selected with an approximate distance of 250 meters, representing its closest surroundings in terms of land use and vegetation. A GPS unit was used to decide the positions of all points and creating a simple map of the area. After the points were chosen the soil moisture investigation began. The soil moisture was evaluated at two depths. The limited number of depths was due to the limitations of the equipments and the models used.

2.2.1 Mapping

The surrounding environment of the field station could be defined as dry farmland, characterized by sand dunes altered with cultivated zones. Figure 6 shows a simple map of the area and the studied points. The studied points are described in Table 1. The appearance of the cultivated fields in the area was roughly estimated with a GPS-unit by using its tracking function around each field. A digital map was then created by linking the coordinates. A polygon was constructed to enclose the investigated area and to estimate the proportion of land use. Approximately 14 % of the area was cultivated. The remaining area was considered to consist of dry sand. All digital mapping was performed in the GIS-software ArcGIS.

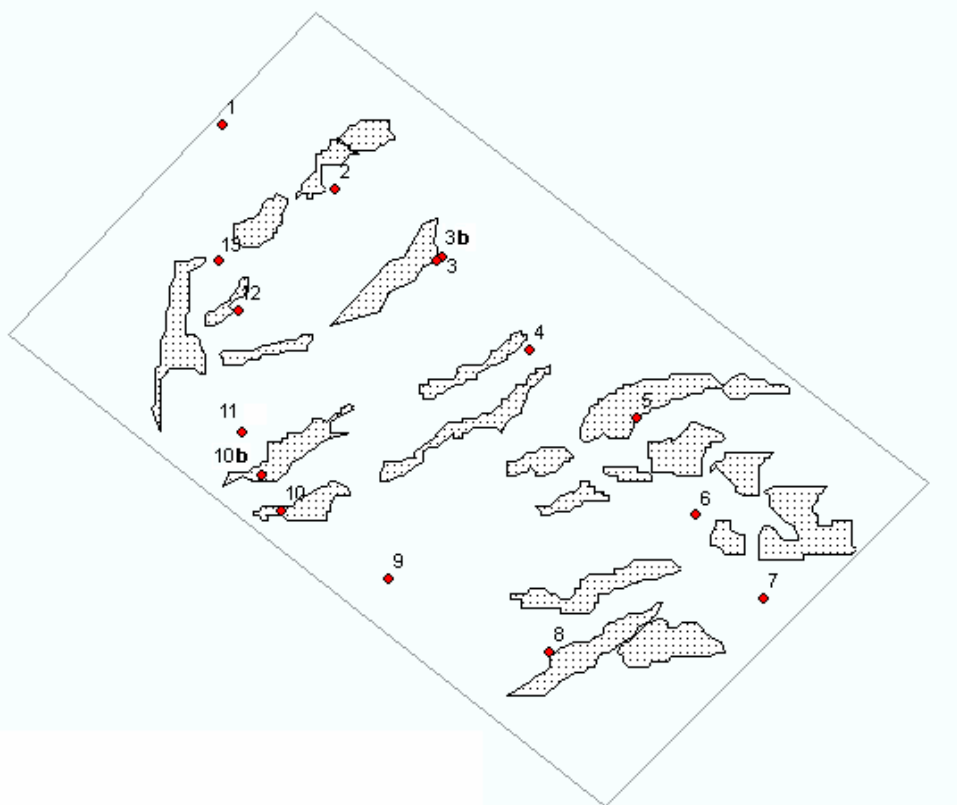


Figure 6. The investigated quadrilateral at the field station. The dotted areas represent cultivated areas. Number 1-13 represent the measure points. Point 3 and 10 was moved resulting in points named 3b and 10b respectively.

Table 1. Summary of the investigation points

Point	Description
1	Located in a ploughed but uncultivated field surrounded by sand, some trees and houses. See Figure 7.
2	Located on a sand dune. Surrounded by cornfields and some trees. See Figure 8.
3	Located among some trees close to a corn field. The soil here was rather hard. See Figure 9.
3b	The measuring point was later moved 20 m away from the trees, since neither the PVC-tube nor the drill could penetrate 30 cm into the soil. This Point was called 3B.
4	Located on a sand dune, vegetated with some shrubs. Cornfield located within 30 meters. See Figure 11.
5	Located in a large cornfield. See Figure 10.
6	Located on sand. Ground covered with different kinds of grasses and bushes. Surrounded with cornfields. See Figure 12.
7	Located on sand, close to some bushes. Surrounded by uncultivated farmland.
8	Trees, poplars.
9	<i>Artemisia Ordosica</i> , shrubs. Figure 14
10	Cornfield, cultivated.
10b	When the cornfield at point 10 was harvested the measuring point was moved to a nearby still growing cornfield.
11	Ground level plants.
12	<i>Hedysarum multijugum maxim</i> , shrub. See Figure 13
13	Ground level plants



Figure 7. Point 1. Ploughed uncultivated land.



Figure 8. Point 2. A dry sand dune.



Figure 9. Point 3. Close to a corn field.



Figure 10. Point 5. Located in a large cornfield.



Figure 11. Point 4. Located in dry sand.



Figure 12. Point 6.

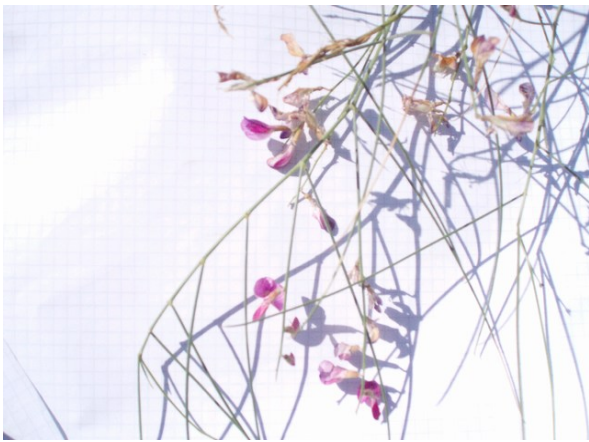


Figure 13. *Hedysarum multijugum maxim*, a shrub present within the area



Figure 14. *Artemisia Ordosica*, a typical shrub for the area.

2.2.2 Soil Moisture Measurements

Soil moisture was examined within two layers. The first layer, comprising the surface soil, was at the depth of 0-10 cm, corresponding to the top Noah layer. The second layer was at the depth of 10-30 cm, which was the largest depth reached with the waveguides.

The soil moisture survey was intended to be performed solely using a Time Domain Reflectometer (TDR), because of its ability to quickly estimate soil moisture in the field. A TDR was supplied by the GS-CIET. This equipment broke down the 8th of September, after only three days of usage. The only available method for soil water measurement was to collect, weigh and dry soil samples. Two soil sampling techniques were tested during the days of 13-15 of September. The intention was to get undisturbed soil samples for each layer. Advantages and disadvantages were compared before the drill was chosen for further usage since the deformation of the PVC tube was considerable. The soil samples were then weighed homogenized before a smaller fraction of it was dried at 105° C during 12 hours and then reweighed. The measured dry density was used to find the retrieved volume and volume percentage of soil moisture. See Figure 17.

2.2.2.1 TDR

The TDR-equipment Figure 15 was supplied with waveguides of two lengths; 15 and 30 cm. The soil water content could therefore be estimated as averages of the two depths of 0-15 and 0-30 cm respectively. In order to achieve a mean soil moisture value for the surface layer (0-10 cm), the waveguides of 15 cm was inserted into the soil with a 45° angle, giving the soil moisture content for 0-10 cm. The 0-30 cm sample was manipulated to account for the depth of 10-30 cm. At each measuring occasion time was noted to simplify further comparison with the simulated results.

The equipment broke down before it was calibrated for this soil type, which is considered as a source of error and will be further discussed in Chapter 2.3.6.3.



Figure 15. The Time Domain Reflectometer with its waveguides and TDR usage in cornfield.

2.2.2.2 Soil Sampling with PVC tube

A 40 cm PVC-tube was used to get a soil sample with intact soil profile. The tube was forced 30 cm into the ground before carefully taken up. The sample was then divided into two samples, one for the upper 10 cm and the other for the lower 10-30 cm. The partitioning was performed with a ruler. See Figure 16. The upper and lower profile could be considered as isolated from each other since the samples were always moist enough to remain intact in the tube. It was also very easy to judge whether the bottom surface looked intact or not. Both samples were carefully scraped into plastic bags, one centimetre at the time. The plastic bags were then sealed to conserve the moisture of the sample.



Figure 16. Collecting soil samples with a PVC tube.



Figure 17. The scale and oven used for water content determination.

2.2.2.3 Soil Sampling with Drill

This method was quite similar to the PVC-tube. Soil was collected in a 20 cm long hollow cylinder at the bottom of the drill and could then be scraped into plastic bags. The bags were sealed and studied, using the scale and oven. The drill was driven down into the soil three times. The first gave the 0-10 cm layer. The bottom surface of the sample was often uneven and difficult to get up so the drill was driven down to 15 cm and the bottom 5 cm were removed before the sampled was sealed.

To get a soil sample for the second layer, the top 10 cm were excavated right next to the first sampling site. The drill was then driven down twice to the total depth of 35 cm in the same hole. Again, the bottom 5 cm was removed before the sample was put and sealed in a plastic bag. See Figure 18.



Figure 18. Extracting soil samples by drill. The ruler was used to get to the correct depth.

2.2.3 Density Measurements

The PVC tube and drill method required the dry density to estimate soil moisture. Dry density was approximated at 0-10 and 10-30 cm by using a 100 cm³ metal container, constructed to give undisturbed soil samples. The container was 5 cm deep and in order to get soil samples from the middle of both soil layers we had to dig down to 2,5 and 17,5 cm depth in the soil, where the samples were collected at each of the 13 measuring points. For each sample the container was forced down to the correct depth, sealed by a lid and then resurfaced by shovel. Since the sample was considered undisturbed with a specific volume the density could be approximated by drying the sample in the container and use the scale to get its mass.

2.2.4 Data Post Processing

Since measuring points 3, 5 and 10 were within cultivated areas, these were estimated as representative values for 14 % of the square. The remaining 10 locations represented sand dune soil moisture and 86 % of the square. Every point with a measured value was used to create the weighted moisture value for that day, using formula (1) below.

$$SM_{daily} = \frac{\sum SM_{cultivated}}{n} \cdot 0.14 + \frac{\sum SM_{sand}}{m} \cdot 0.86 \quad (1)$$

where n is the number of soil moisture measurements at cultivated points for that day and m is the number of measurement at sand points. The same formula was used for both depths.

2.2.5 Meteorological Recordings

At the field station the China Agriculture University (CAU) had a weather station collecting hourly values of precipitation, temperature, potential evaporation and wind speed. Data between the 3rd and 29th September was used to get estimations of temperature variations and precipitation. This equipment was used to get the annual precipitation amount as well.

In order to interpret the data in a statistical context, complementary data was retrieved from the world climate data base³⁴. The chosen station Minqin is located nearby with a similar elevation and was presumed to climatically agree with the Wuwei area. This data was recorded at 38.63°N 103.00°E and 38.72°N 103.10°E between 1953 and 1990. CAU is also conducting desertification related experiments at a station in the Minqin area.

Our soil moisture measurements were compared with satellite derived atmosphere and soil parameters of 1 x 1 degree spatial and 6 hours temporal resolution. Soil moisture parameters were given in two layers 0-10 and 10-40 cm. The data was provided by the Data Support Section of the Computational and Information Systems Laboratory at the National Center for Atmospheric Research (NCAR, USA). NCAR is supported by grants from the US National Science Foundation. Data was collected by the National Weather Service and can be retrieved from the NCEP website³⁵. Daily mean values were acquired by using GrADS (See chapter 4.4.2).

2.2.6 Sources of Error

2.2.6.1 Scale

The scale had up to 0.4 g difference between measurements for the same sample. This could be an effect of unreliable power supply or scale quality. It does however seem likely that the plastic bowl used in the procedure got torn out by repeated cleaning. This error would create overestimated soil moisture values.

Sometimes the weighing had to wait for several hours due to power failure. The samples were kept as cool as possible, but it is likely that some water was lost during this time. The oven was supposed to dry the samples at 105° C for 12 hours but did often turn off due to lack of power. These would result in underestimated soil moisture values. The problem with power failure during the drying phase was usually compensated with a longer drying time.

2.2.6.2 TDR

The TDR was never calibrated, which should be a necessary procedure to interpret the reflection time to correct soil moisture. Calibration is especially important in saline soils like these, where the ions in the soil will give a slower reflection. This results in an overestimation of soil moisture. The error is usually not more than 2% for most soils, according to the TDR user's manual.³⁶

³⁴ World Climate, 2005

³⁵ NCEP, 2007

³⁶ Soilmoisture equipment corp., 1996

2.2.6.3 PVC method

Soil from both layers was taken at the same time with the PVC tube. There was an uncertainty when separating the soil in the tube into two bags.

2.2.6.4 Drill Method

Dry surface soil tended to fall in the hole and mix up the profile when the drill was pulled up. This was especially true when the top soil was very dry. In many cases the top soil was too dry to even stay in the drill.

2.2.6.5 GPS

The manufacturer of the equipment states that the given coordinates have an uncertainty of up to 300 meters. This error is larger than the intended distance between the measuring points. It is common in GPS application and can be solved with a reference point of known location. This could however not be found. The points relative positions have an error of up to 10 m.

2.2.6.6 Metrological Recordings

Due to power failure the equipment was down March through April. This affected the measurement of the annual precipitation for 2006. The amount of precipitation for these months is usually low, according to NASA, 8 mm fell during the period.³⁷ This error is unaccounted for.

2.3 Results and Discussion

The field collected parameters could be viewed in Figure 19 below together with the NCEP estimations of soil moisture. Average soil moisture in the top layer is 6.6 % and 11.8% in the deeper layer. All soil moisture measurements can be found in Appendix III.

The NCEP soil moisture is significantly higher and less fluctuating than our measurements. The NCEP estimation covers a 100 x 100 km square and can not be seen as a full representation of the Wuwei area. The static appearance is explained with the large coverage which can offset local precipitation events. The variables are generalized for the whole square and do not show local differences. The bottom layer has higher soil moisture levels than the top layer for both NCEP and our measurements. The NCEP data indicates an increase of 0.4 % in the bottom layer.

Five rain events took place during our stay (3rd – 30th September), adding up to 17 mm of precipitation. The total recorded precipitation for 2006 was 189 mm. Climatologic data for the region states that the average September precipitation is 16 mm and average yearly precipitation is 110 mm. It seems like September was a typical month in a rainy year. Most precipitation fell in late July to mid August.

³⁷ NASA/GIOVANNI, 2007

Average temperature during our stay was 13.1 °C with a daily average maximum temperature of 24.6 °C and daily average minimum of 4.1 °C. Statistical average September temperature is 16.0 °C, average daily maximum and minimum temperature is 23.5 °C and 9.0 °C respectively. This indicates a slightly colder September than usual.

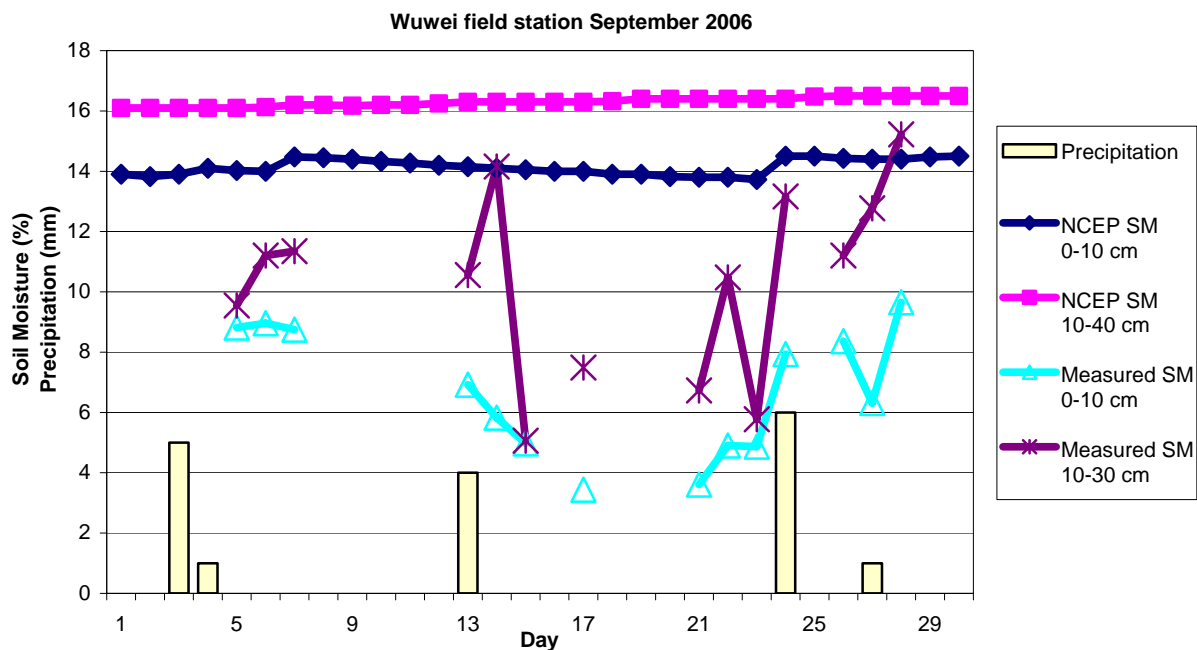


Figure 19. Field measurements at the Wuwei field station during September 2006. Soil moisture is weighted averages for the two depths, 0-10 and 10-30 cm. Satellite observed soil moisture is noted as NCEP SM.

3 Environmental Modelling

The required input data for LIS modelling has not been available. The NASA server was down due to system maintenance during spring 2007 hindering simulation of September 2006 and model validation. Instead, the investigation focused on LIS modelling in retrospect using older data sets. Measured soil moisture values from this period of time are hard to find, so no validation has been made. The two Land Surface Models were rather compared and investigated than evaluated.

The study consists of two parts, where the first part is focused on configuration of the model and the second on soil moisture studies.

For the first part the following are studied:

- How well does LIS interpret precipitation from the forcing data?
- Which forcing data set gives the better precipitation results?
- How will the initial soil moisture affect the soil moisture simulation?

For the second part soil moisture patterns are studied in two scenarios:

- In the first scenario the four year period January 1st 2000- January 1st 2004 is studied for LSM differences and local differences in the Shiyang area.
- The second scenario is constructed to study the infiltration process in the two LSMs.

4 LIS Description

As previously mentioned LIS is developed to perform modelling at high spatial and time resolution and is currently supporting land surface simulations with 1×1 km resolution. Figure 20. All instructions and settings for a LIS simulation are given in the lis.config file (See Appendix IV). When a simulation is launched the LIS core will create a spatial and temporal domain in which the simulation will run. Then soil and vegetation parameters and initial conditions are read and set according to the configuration. The LIS core will then find the correct forcing input file and create interpolations to fit the resolution of the LIS domain before the computing is initiated by calling the selected LSM. This is done grid cell by grid cell until the domain is completed. Output data is written after each time step as well as a text summary of maximum, minimum, standard deviation and mean value of the output parameters. LIS will read the next input data file when necessary. A summary file can be found in Appendix IV. LIS writes a restart file after each day. This file can be used when making a new simulation over the same area, instead of setting initial parameters.

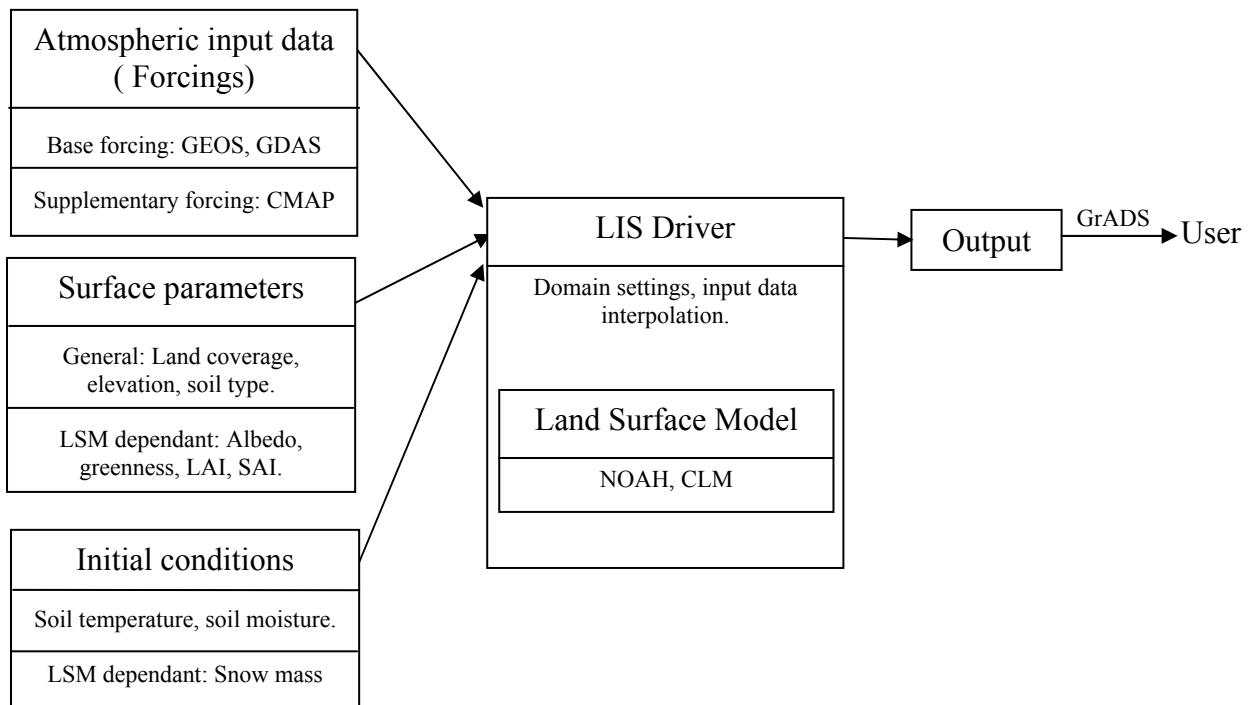


Figure 20. LIS overview

The LIS software is free and available for download at the LIS website. LIS version 4.3.1 was used for all simulations. There has however been a release of version 4.3.2 and a pre-release of version 5.0 since our tests were started.

4.1 Land Surface Models (LSM)

The land surface model (LSM) calculates water and energy related parameters explaining the land surface condition. The soil-vegetation-atmosphere-interaction is interpreted with one-dimensional equations governed by the fundamental requirement of conservation of mass and

energy. Based on atmospheric forcings and given initial conditions, the surface state parameters are derived for each grid cell at each time step.

In the investigated version of LIS two LSMs are available, CLM and Noah. CLM and Noah are both very complex models with slightly different land surface schemes and equations. Generally, Noah and CLM are based on the conceptualized idea that the land surface could be expressed by the three sub-units; the canopy, the snowpack and the soil profile. Figure 21.

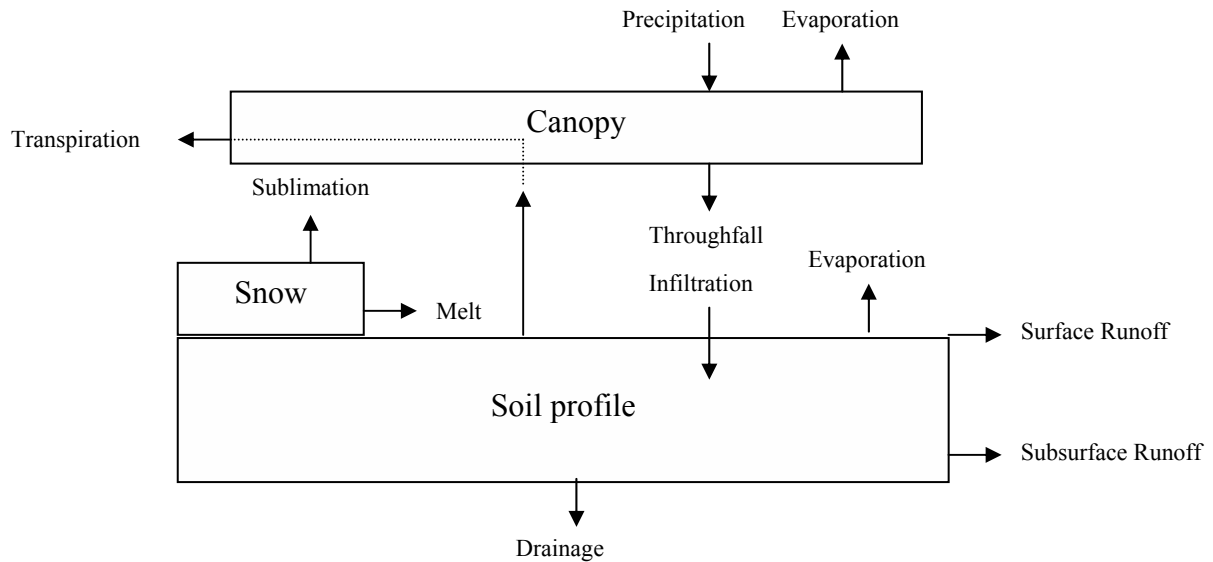


Figure 21. Conceptual understanding of the LSMs Noah and CLM.

The soil profile is influenced by surface and subsurface runoff, infiltration, evaporation and transpiration through the canopy. Since soil moisture is the main focus in this study, the soil column with its similarities and differences will be explained a bit further for both LSMs.

4.1.1 Noah

The currently used version in LIS is Noah 2.7.1. Noah is an acronym after its creators, a collaboration between; National Centers for Environmental Prediction (NCEP), Oregon State University (OSU), U.S Air Force Weather Agency and Research Lab and Hydrologic Research Lab at National Weather Service.³⁸

The Noah soil profile has a total depth of 2 meters. The three top layers (with a thickness of 0.1, 0.3 and 0.6 m) represent the root zone affected by vegetation with the fourth layer (with a 1m thickness) acting as a reservoir with gravity drainage at the bottom.³⁹ This is based on a soil vegetation model created by Pan and Mahrt (1987)⁴⁰ which was further developed by F. Chen et al. (1997).⁴¹

³⁸ Mitchell, K., 2001

³⁹ Chen, F., et al., 1997

⁴⁰ Chen, F., et al., 1996

⁴¹ Ek, M. B., et al., 2003

Vertical flow in Noah is derived from Darcys law and is known as the Richards equation (1931)⁴². Hydraulic properties are based on the scheme developed by Cosby et al. 1984. Infiltration and runoff is based on the Simple Water Balance (SWB) scheme described in Schaake et al. (1996) and potential evaporation is developed by Mahrt and Ek (1984) with changes for bare soil evaporation of Betts et al. (1997).⁴³

Initial soil moisture is defined as the volume percent of soil moist (v%), mm³ water per mm³ soil. Output data is written hourly in Noah.

4.1.2 CLM

The Community Land Model (CLM) version 2.0 is used in LIS. This LSM is created by collaboration between Terrestrial Sciences Section (TSS), Climate and Global Dynamics Division (CGD), National Center for Atmospheric Research (NCAR) and CCSM Land Model Working Group.⁴⁴

The soil column is described with ten layers in CLM, down to the total depth of 3.43 meters. The top layers are just a couple of centimetres thick and the deepest layer, layer 10, is 1.13 meters.

Vertical water flow is, as for Noah, described with Richards equation (1931)⁴⁵. The hydraulic properties vary with volumetric water content and soil texture according to Clapp and Hornberger (1978) and Cosby et al. (1984).⁴⁶ Runoff is estimated from unsaturated and saturated areas for both surface and subsurface runoff. Surface runoff is a combination of Dunne runoff from saturated areas and a scheme developed by Dickinson et al. (1993) from unsaturated zones. Subsurface flow is characterized as bottom drainage, lateral base flow due to topography and saturation excess.⁴⁷ Lateral base flow and saturation excess is approximated from layer 6-9.⁴⁸

The initial soil moisture is defined as the initial field capacity fraction. The field capacity is the maximum water holding capacity of the soil and therefore depends on the soil composition. Output data is written every three hours in CLM.

4.3 LIS Input

LIS requires two kinds of globally gridded data; atmospheric forcings and parameter data.

4.3.1 Atmospheric Forcings

The data sets needed for LIS simulations could be divided into mandatory base forcings and optional supplementary forcings. The forcings could be satellite observed, gauged, model

⁴² Chen, F., et al., 1996

⁴³ Ek, M., et al, 2003

⁴⁴ NCAR, 2007

⁴⁵ Oleson, K., and Dai, Y., et al 2004

⁴⁶ Dai, Y., et al., 2003

⁴⁷ Ibid.

⁴⁸ Oleson, K., and Dai, Y., et al 2004

derived or a combination. The data sets could include different variables and vary in spatial and temporal resolution. The LIS driver is then to interpolate resolution and time step given by the forcings to the appropriate dimensions for a LIS run.⁴⁹

All data sets could be treated individually in GrADS as well as being input to LIS for further simulation.

4.3.1.1 Base Forcing

The base forcings provide the model with all necessary data about the atmosphere state, such as precipitation and radiation. LIS has the possibility to run with several base forcing options but only two have been tested. These are; Global Data Assimilation System (GDAS) and Goddard Earth Observing System (GEOS).⁵⁰ Both sets have a global coverage and consist of model derived meteorological data. The temporal resolution is three hours for GEOS and six hours for GDAS.⁵¹

The GDAS set is produced by the National Weather Service's National Centre for Environmental Prediction (NCEP).⁵² The set include 23 parameters. Data was available from 1:th of January 2000 until 29:th of July 2004. It was however divided into two different resolutions GDAS1 and GDAS2. The first period until 29:th of October 2002, is represented by GDAS1, which has a spatial resolution of ≈ 0.7 degrees. GDAS2 covers the remaining time period with the finer resolution of ≈ 0.47 degrees.

GEOS assimilated data set is created by NASA, and has a temporal cover from 19:th of December 2000 until 12:th of November 2003. GEOS switch resolution in September 2002 contributing to two different data sets; GEOS323 and GEOS4. The resolution changes from 1×1 degree to 1.25×1 degrees. GEOS323 has 15 parameters, which is changed into 16 in GEOS4.

A one month sample of GEOS and GDAS data for June 2001 is available at the LIS website after completed registration.

4.3.1.2 Supplementary Forcings

The supplementary data sets in LIS are optional and work as a complement to the base forcings. Supplementary forcings consists of meteorological and soil related model derived parameters that could contribute with finer information regarding, for instance, radiation or precipitation. NOAA's Climate Prediction Centre (CPC) Merged Analysis of Precipitation (CMAP) is such a forcing set, providing information of precipitation.⁵³ CMAP had a global coverage with a temporal resolution of 6 hours. CMAP is available during the period of January 2001 until January 2004. The spatial resolution varies from ≈ 0.7 degrees until 29:th of October 2002, to ≈ 0.47 degrees. Like the GDAS set a change in resolution occurs in October 2002. When supplementary forcings are included in a LIS run, the parameter value from this forcing is chosen prior to the same parameter supplemented by the base forcing.

⁴⁹ NASA/GSFC, 2004

⁵⁰ NASA/GSFC, 2007

⁵¹ NASA/GSFC, 2007a

⁵² NOAA, 2004

⁵³ NOAA, 2002

4.3.2 Parameter Data

LIS needs specific information about the earth surface in order to operate properly. This information is provided as data sets of land surface parameters, divided into sets that are required by LIS in general, and into sets that are LSM specific.

All models need information about the land coverage, vegetation classification and soil properties. The land mask is provided by the University of Maryland (UMD) with 1 km resolution, separating land from water. The vegetation set is also provided by UMD with a 1 km resolution. Here every grid cell is categorized between 0-13 depending on land cover. For the UMD vegetation classification see Appendix IV.⁵⁴ Specific soil properties for this study were obtained via the Food and Agriculture Organization (FAO) digital soil map of the world (SMW).⁵⁵ The FAO set is provided by NOAA and consists of information about soil color and soil fractions of sand, silt and clay.⁵⁶

Depending on which LSM is used in the LIS run, data sets need to be altered or added. Noah needs additional data sets about; bottom layer temperature, greenness fraction, surface albedo and maximum snow albedo. These data sets have different temporal coverage. Bottom layer temperature and maximum snow albedo are static while greenness fraction and surface albedo follow the seasonal changes. Noah also uses a further classification of soil and vegetation types. The FAO soil fraction data is used to define the soil class of each grid cell. There are nine classes, each with specific hydrological properties.

CLM uses monthly stem and leaf area indices (SAI and LAI) to understand the annual changes in vegetation properties. Two additional files define the canopy height and vegetation parameters for each vegetation class.

All the parameter data is possible to be downloaded at the LIS website after registration.

4.4 LIS Requirements and Software

LIS demands a lot of computing and storage resources to run simulations. The full output for a one year CLM simulation needs 71 TB of disk space, GDAS base forcing data requires about 18 GB / year and the necessary parameters for both NOAH and CLM require 113 GB. A one day LSM simulation for a single grid cell is expected to take no more than 0.4 ms. However, this adds up to billions of calculations for a larger catchment, which takes days or even weeks unless powerful processors are used. LIS is programmed for parallel computing, which means that several processors calculate different parts of a common task.

4.4.1 Lunarc

We used the Lunarc network to run LIS remotely. Lunarc is a centre for scientific computing in the southern region of Sweden and it has been active since 1986. We normally used four processors of the Docenten cluster to run the simulations. Docenten consists of 210 AMD

⁵⁴ UMD, 2006

⁵⁵ NRCS, 2007

⁵⁶ NOAA, 2007

processors, model Opteron 148; which implements the x86-64 architecture. Each processor is running at 2.2 GHz.⁵⁷ The LIS software and all input and output data was also stored at the Lunarc system.

4.4.2 GrADS

The Graphical Analysis and Display System (GrADS) is a software tool used for manipulation and visualization of geographical scientific data. A user defines what data and dimensions that are included in the data set in a .ctl-file (see Appendix IV) The software is developed by the Institute for Global Environment and Society (IGES). GrADS understands FORTRAN scripts which facilitates execution of dense operation sequences. GrADS was used to access, study and convert binary data into a more comprehensible format. GrADS is available for free download at IGES webpage.

⁵⁷ LUNARC, 2007

5 Statistical Approach

LIS simulated or isolated forcing values were compared with the actual station measurements. The deviation between the registered precipitation and the simulated, or forcing isolated, acted as a measure of operational capability.

The deviation was defined in two terms; total absolute error, E , and the sample correlation coefficient, r .

5.1 Mean Absolute Error, MAE

The mean absolute error, MAE , was defined as:

$$MAE = \frac{\sum_{i=1}^n |y_{1,i} - y_{2,i}|}{n} \quad (2)$$

where $y_{1,i}$ is the simulated/isolated value at the same location and at the same time $y_{2,i}$ is the actual measurement at a given time and n is the number of measurement in the series

5.2 Total Error

The total error is calculated in a similar way as the mean absolute error.

$$E = \sum_{i=1}^n (y_{1,i} - y_{2,i}) \quad (3)$$

A positive error means that the model has made an overestimation.

5.3 Sample Correlation Coefficient, r

In order to estimate a correlation between two series of measurements Y_1 and Y_2 the sample correlation coefficient, r was used. A value between -1 and 1 is possible where 1 indicates a perfect correlation and -1 an inverse correlation, i.e. the value in one of the data collections is high while the other collection is low or vice versa. The correlation coefficient was defined according to:

$$r(y_1, y_2) = \frac{\sum_{i=1}^n ((y_{1,i} - \bar{y}_1) \cdot (y_{2,i} - \bar{y}_2))}{s_1 \cdot s_2 \cdot (n - 1)} \quad (4)$$

where \bar{y}_1 , \bar{y}_2 , s_1 and s_2 are the mean values and the standard deviations of y_1 and y_2 .⁵⁸

⁵⁸ Box, G., 1978

6 Simulated Area

The area studied in LIS was the Shiyang river basin. Thirteen points in the region were studied. Some were chosen because of existing precipitation data and some due to climate and land use properties. The river basin was divided into three zones with different topological and hydrological characteristics, based on classifications by S. Kang. The altitude and precipitation decreases from south to north. Zone 1 in the south, is characterized by the Qilian Mountains being the highest and most humid and zone 3 in the north being the driest and lowest. See Figure 22. The classification is made using a digital topographical map in ArcGIS. Another digital map of land use was utilized to determine specific land conditions at the studied coordinates.

6.1 Precipitation Data

In order to evaluate the performance of LIS, validation data was required. Two sources supplied the investigation with precipitation measurements; Hydrological Bureau of Gansu, and China West.

6.1.1 Precipitation Validation Data; Hydrological Bureau of Gansu

Station named, Hongyashan, Huangyang, Jiutiaoli, Nanying and Xiahe were received from Hydrological bureau of Gansu. Each hydrologic station contributed with monthly precipitation and evaporation values during the year 2000 and 2001. Only precipitation was studied. Monthly averages can be found in Appendix II.

6.1.2 Precipitation Validation Data; China West

China west supplied information for the stations named with numbers; 52674, 52679, 52681 and 52787. Several parameters were available as daily values, but only precipitation was used. A 30-day-loop added 30 days of precipitation to represent monthly values. The loop started at the first day every month summarizing 30 days ahead, giving a generalization of the precipitation of that month. China West supplied data from January 2001 through December 2003. Monthly averages can be found in Appendix II.

6.2 Shiyang Soil Moist Survey

The nine previously mentioned points were studied in the soil moisture investigation together with three additional points; desert, meadow and wetland. These were selected because of interesting properties in terms of land use and location. The point named desert and wetland are both located in Zone 3 and were studied to compare similarities and differences in soil moisture behaviour for different land uses. These points have no measured values but are simply studied for their properties. A brief summary of all 13 investigation points could be viewed below in Table 2. Their location in the watershed could be viewed in Figure 22.

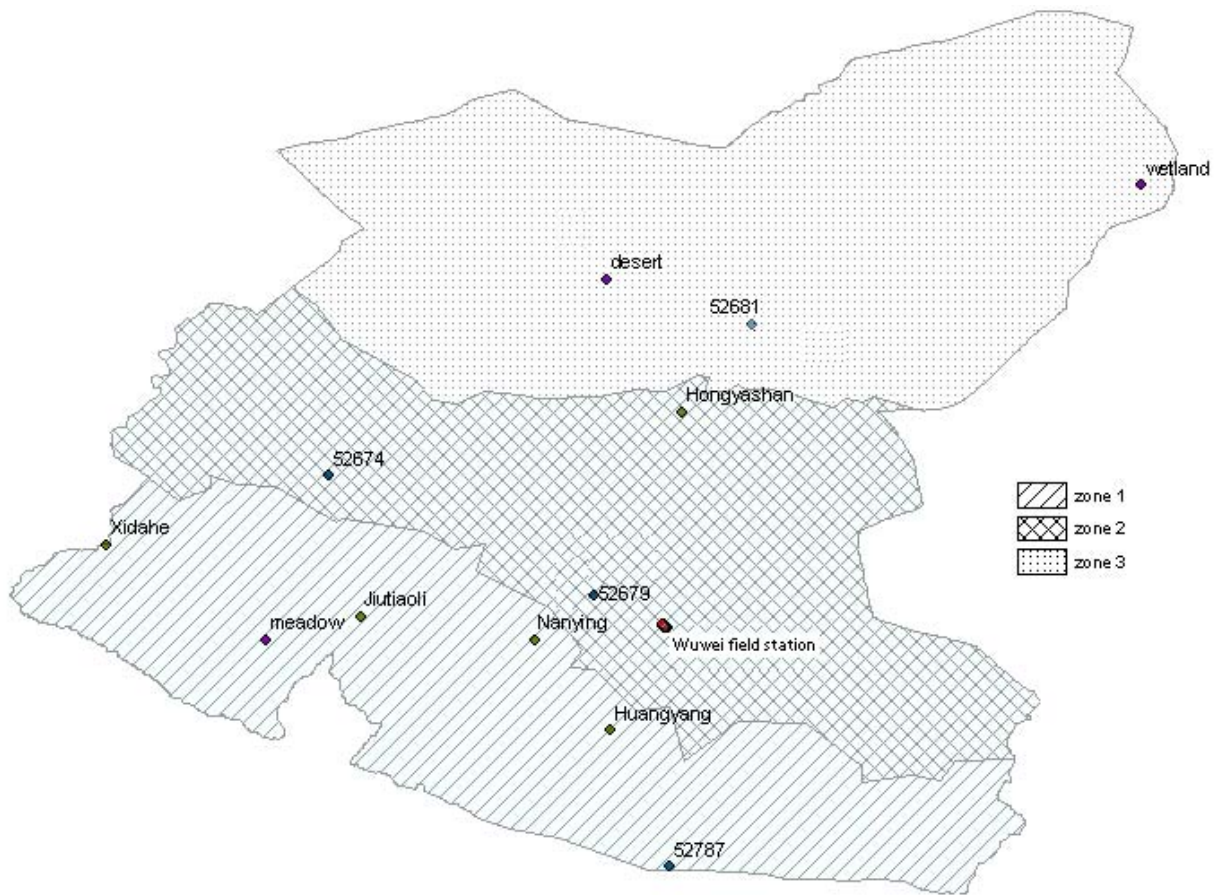


Figure 22. Shiyang with the investigation points.

Table 2. A summary of all investigated points

Station	Location latitude	Location longitude.	Height Zone	Land use	Measured Parameter	Period	Source
52674	38.23	101.97	2	Urban	P	2001-2003	China West
52679	37.92	102.67	2	Dry Farmland	P	2001-2003	China West
52681	38.63	103.08	3	Urban	P	2001-2003	China West
52787	37.20	102.87	1	Dry Farmland	P	2001-2003	China West
Hongyashan	38.40	102.90	1	Dry farmland	P	2000-2001	Hydrological Bureau of Gansu
Huangyang	37.56	102.71	2	Dry Farmland	P	2000-2001	Hydrological Bureau of Gansu
Jiutiaoli	37.86	102.05	1	Woodland	P	2000-2001	Hydrological Bureau of Gansu
Nanying	37.80	102.51	1	Meadow	P	2000-2001	Hydrological Bureau of Gansu
Xidahe	38.05	101.38	1	Rural Residential	P	2000-2001	Hydrological Bureau of Gansu
Wuwei	37.83	102.85	2	Dry Farmland	P, SM, T	Sept. 2006	Field studies
Desert	38.75	102.70	3	Desert	-	-	-
Meadow	39.00	104.11	1	Meadow	-	-	-
Wetland	37.80	101.80	3	Wetland	-	-	-

7 LIS Methodology

The simulated area was set as latitude 37.155 – 39.445 °N and longitude 100.995 – 104.195 °E in all cases except if stated otherwise. This box includes the Shiyang river basin and all investigated points. LIS version 4.3.1 was used for all simulations. The unit used for soil moisture studies is always v%, unless stated otherwise.

7.1 Configuration and Set Up

In order to make reliable simulations the model needs a good configuration. Forcing options and initial values were altered and compared in order to find strengths and weaknesses. The forcing data is of about 50-100 times lower in resolution than the LIS grid, so all data is interpolated before used in LIS calculations. The investigation also included evaluation of the LIS interpolation tool.

7.1.1 Forcing Precipitation Validation and LIS Interpolation Evaluation

This part of the investigation was performed with the intention to find the best forcing option, based on validation of the precipitation parameter. Precipitation data after LIS interpolation was extracted and compared with observed data. Isolated data from the raw base forcing sets was also extracted and compared with observed values.

7.1.1.1 LIS Precipitation Interpretation

Three LIS runs were performed over the Shiyang area for the time period January 1st 2001 – January 1st 2004, one with GDAS, one with GEOS and one with CMAP as precipitation source. LIS interpretation of precipitation is implemented separately before further treatment in the land surface modelling procedure and therefore choice of LSM was of no significance in this investigation. Noah was chosen for all simulations. GDAS was used as base forcing in the CMAP run. The results were then retrieved with GrADS.

7.1.1.2 Data Retrieval from Forcings

GDAS and GEOS base forcing and CMAP supplementary forcing were all available for the time period 2001-2003. GrADS was used to retrieve monthly precipitation values from each forcing data set at the nine locations.

7.1.1.3 Data Comparing

The resulting precipitation from the three simulations was compared with actual measurements to find differences between them. The isolated raw forcing values were also compared with the measurements, in order to compare the data before and after interpolation. Comparisons were made in terms of r, mean and total error. All comparisons were made at the nine stations from our two sources; China west and Hydrological bureau of Gansu. China west supplied

measurements during the entire period while stations provided by the Hydrological bureau of Gansu were only representative during year 2001.

All locations were extracted using its corresponding coordinate with the exception of Hongyashan. Since this station was positioned next to a reservoir, the UMD mask classified the area at Latitude 38.40, Longitude 102.90 as water. Since the models only simulate land the grid cell is excluded from LIS. Instead, a close by coordinate (Latitude 38.43, Longitude 102.90) was chosen to represent Hongyashan.

7.1.2 Spin Up Test

Soil moisture in the entire profile and area is initially represented by only one value. This is far from the truth and the rough estimation of soil water content displaces the equilibrium equations resulting in a delay of correctly simulated parameters. This phenomenon is known as the spin up effect. For instance CLM needs several decades of simulations to get accurate simulations of the deeper layers.⁵⁹ In order to minimize this effect it is important to get an initial soil moisture value that decreases the spin up time as far as possible. In this investigation LIS was run at two locations for both LSMs. The chosen locations were the station with the least precipitation, station 52681, and the station with the most precipitation, station 52787.

Table 3. The initial soil moisture values chosen for the two LSMs at the different locations.

Location	Noah	CLM
52681	0.05	0.1236
52681	0.20	0.4944
52681	0.35	0.8652
52787	0.05	0.1263
52787	0.20	0.5052
52787	0.35	0.8842

The soil moisture data given from GDAS indicated a mean soil moisture of 0.23 for the entire region. The models were tested with initial soil moisture at 5, 20 and 35 volume percent. The conversion to find corresponding CLM soil moisture values was made by trial and error, due to the difference in the initial soil moisture definitions. The initial values used could be observed in Table 3.

To find whether a model is spun up or not, the shapes in the simulation results were studied by looking for “natural” annual cycles or if there seemed to be a trend of annual increase or decrease of moist. This method is of course imprecise but can give an indication of how the initial soil moist influences the spin up time.

7.2 Soil Moisture

Since no measured soil moisture values were available, this study is based on simulated values only. Differences in soil moisture patterns were compared for the two LSMs in two tests; a four year simulation and a created rain event. The first scenario aimed at pointing out differences in annual behaviour and land use and therefore included all investigation points within Shiyang. The latter aimed at investigating infiltration patterns and was performed in Wuwei solely. Because of the results from the precipitation tests, GDAS without CMAP was used in the soil moisture tests.

⁵⁹ Vertenstein, M. et al, 2004

7.2.1 Comparison of Noah and CLM Over a Four Year LIS Run

In this test the LIS model was run twice from January 1st 2000 – January 1st 2004, once with Noah and once with CLM. The initial soil moisture was set to 0.25 in Noah and 0.64 in CLM. The initial temperature was set to 272.2 K for both runs. This value was based on the catchments mean soil temperature estimated from the GDAS forcings at the starting date. The initial snow mass was set to 0 for the CLM run.

The varying soil profile interpretation, with four layers in Noah and ten in CLM, required transformation for intercomparison reasons. The CLM levels were therefore transformed into the corresponding depth and thickness of the Noah-layers. E.g. the combination of Layer 4, Layer 5 and 50% of Layer 6 in CLM corresponds with Noah Layer 2. Layer 10 in CLM was excluded completely. The conversions are described in Table 4 and Figure 23.

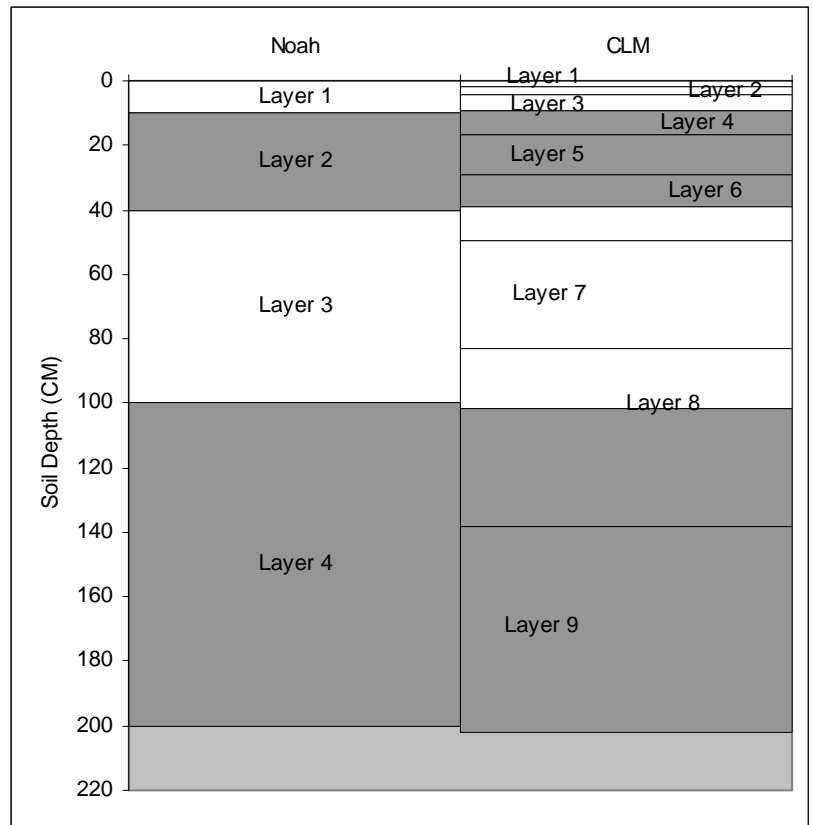


Figure 23. The Noah and CLM layer depths. The combinations of CLM Layers are shown in white and gray.

Table 4. The layers in the two LSMs and the combination of CLM layers into matching Noah depths.

	Noah Layer Thickness (cm)	CLM Layer Thickness (cm)	CLM Layer Combinations	CLM Layer Combination Thickness (cm)
Layer 1	10	1.75	Layer 1, 2, 3	9.06
Layer 2	30	2.76	Layer 4, 5, 6 (50%)	30.05
Layer 3	60	4.55	Layer 6 (50%), 7, 8 (33%)	62.25
Layer 4	100	7.5	Layer 8 (67%), Layer 9 (70%)	100.86
Layer 5		12.36		
Layer 6		20.38		
Layer 7		33.6		
Layer 8		55.39		
Layer 9		91.33		
Layer 10		113.7		

7.2.2 Modelling Constructed Rain

According to GDAS forcing data a heavy rainfall occurred in June 2002. This event was combined with a dry period of 23 days that occurred in July 2000 to create an undisturbed rain scenario and study the infiltration behaviour of the two LSMs. 34 mm rain fell in a single event, starting June 6th 2002 and with a duration of 38 hours. See Figure 24. The simulated area was a 11 X 11 km grid, with the Wuwei coordinate as its centre. The simulation started at 0:00 the 6th of June and lasted 48 hours. The rain started to fall at hour 10. The last written LIS restart file from this period was then used in the following simulation of the dry period, from 3rd to 26th July 2000. The initial soil moisture was set to 25 % in the Noah simulation and 58.67 % when CLM was used. This value was found to give an initial soil moisture very close to 25 % in this region. The initial temperature was set to 290 K, based on GDAS estimations. The infiltration process was then studied in the individual layers. In this investigation, all CLM layers were used. The rain event started 10 hours after the simulation began. However, hour 0 is always referred to as the first hour of the rain event.

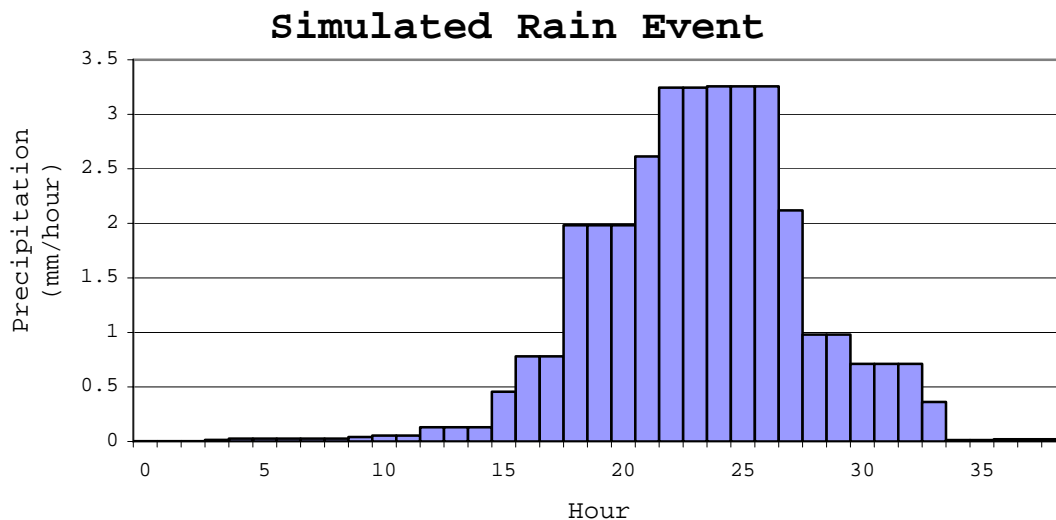


Figure 24. Hydrograph of the created rain event. Precipitation intensity (mm/h) for the rain duration (h).

8 Results and Discussion

8.1 Configuration and Set Up

8.1.1 Forcing Precipitation Validation and LIS Interpolation Evaluation

The performance of the model runs and the forcings are evaluated in terms of sum error E , mean absolute error MAE and r . These numbers are presented below. First for each station individually in Table 5, 6 and 7 then averaged in Table 8. GEOS, GDAS and CMAP are denoting forcing extracted values compared to observed precipitation data. LIS GEOS, LIS GDAS and LIS CMAP are denoting the LIS simulations using the indicated forcing option compared to the observed data.

Table 5. The r correlation values for measured precipitation at each station and the modelled precipitation.

	GEOS	GDAS	CMAP	LIS GEOS	LIS GDAS	LIS CMAP
52674	0.77	0.78	0.86	-0.09	0.90	0.86
52679	0.65	0.53	0.67	-0.01	0.89	0.78
52681	0.63	0.71	0.81	-0.10	0.81	0.84
52787	0.85	0.80	0.78	0.09	0.84	0.82
Hongyashan	0.93	0.75	0.84	0.95	0.86	0.85
Huangyang	0.92	0.84	0.85	0.98	0.87	0.85
Jiutiaoli	0.92	0.93	0.97	0.94	0.96	0.99
Nanying	0.90	0.77	0.82	0.94	0.83	0.87
Xidahe	0.97	0.98	0.98	0.95	0.95	0.97

Table 6. The average of the absolute error for monthly precipitation at each station.

	GEOS	GDAS	CMAP	LIS GEOS	LIS GDAS	LIS CMAP
52674	15.6	9.7	6.7	46.1	6.4	6.4
52679	15.2	13.0	15.9	45.3	11.9	22.7
52681	8.0	8.7	6.2	43.1	5.9	5.3
52787	13.2	16.2	47.7	42.9	18.4	29.8
Hongyashan	3.7	5.4	6.4	3.6	5.6	5.6
Huangyang	11.3	11.0	44.0	7.3	17.9	40.2
Jiutiaoli	6.4	6.4	14.3	9.0	5.9	6.9
Nanying	8.6	13.4	49.3	6.7	14.0	25.4
Xidahe	8.9	17.1	11.3	13.0	9.6	8.3

Table 7. The total difference between measured precipitation and modelled precipitation at each station (mm).

	GEOS	GDAS	CMAP	LIS GEOS	LIS GDAS	LIS CMAP
52674	455	-277	-123	1267	-108	-86
52679	328	-21	312	1327	333	738
52681	40	-290	-189	1304	-114	-97
52787	-15	65	1578	734	231	897
Hongyashan	23	-50	56	-19	-14	2
Huangyang	-135	33	526	-81	190	476
Jiutiaoli	-34	-2	162	-106	48	67
Nanying	-75	93	586	-49	137	294
Xidahe	77	-205	-135	-146	-103	-100

Table 8. The averages of the r- values and the absolute values and the sum of all total errors for all stations.

	GEOS	GDAS	CMAP	LIS GEOS	LIS GDAS	LIS CMAP
Mean r	0.84	0.79	0.84	0.52	0.88	0.87
Mean of absolute errors (mm/month)	10.1	11.2	22.4	24.1	10.6	16.7
Sum of total errors (mm)	664	-653	2773	4231	600	2190

These numbers indicates that GEOS and GDAS give almost equally good performance in terms of error before interpolation. GEOS tends to overestimate the precipitation while GDAS tends to underestimate it. GEOS correlates somewhat better than GDAS to the measurements. CMAP performs well in some points but overestimates the precipitation in others. The poor performance is hard to predict.

The performance is improved when LIS interprets the precipitation data. The exception for this is GEOS at the China West Stations. LIS makes huge overestimations and gives, what looks like, random precipitation, starting October 2002. The reason for this has been traced to the change in data type, from GEOS323 to GEOS4, which occurs that month. The stations from the Hydrological Bureau of Gansu are not affected of this since only year 2001 is evaluated at these stations.

It is obvious that GDAS is the more reliable data forcing to use with LIS during these years and it seems like there is no good reason to use additional CMAP forcing. It should be noted that even though the GDAS values are closer to the measured values after LIS interpretation, LIS has greatly increased the precipitation and turned an underestimation of 653 mm in GDAS into an overestimation of 600 mm.

The strange behaviour of GEOS4 in LIS has been reported to the LIS support group at NASA, but the issue has not been addressed.

8.1.2 Spin Up Test

The results from the runs in two of the layers can be viewed in Figure 25 and 26. These results are representative for many of the other layers. The 35% scenario seems to have a normal fluctuation pattern quite early in the 40-100 cm Noah layer at the wet location. There is a little increase during the first two years for the 20% scenario and what looks like an increase for about three years in the 5% scenario. By studying the scenarios in CLM 9-17 cm at the dry location it seems like there is quicker decrease of soil moist in the 35% and 20% scenarios than the increase in the 5% scenario. The excessive moisture in the 35% scenario is lost just some months after the 20% scenario looks stabilized.

When the two figures are compared it also looks like the spin up time is shorter at a location with much precipitation.

Since soil moisture decrease is quicker than an increase it seems like a slightly higher initial soil moisture is preferable for achieving a short spin up time. The reason for this might be that the potential evaporation in the area is high and the precipitation is low. A wet soil will be affected as soon as the potential evaporation is high, while the drier soil needs precipitation to change.

Initial Soilmoist Scenarios
Noah Layer 3 (40-100 cm), Wet location

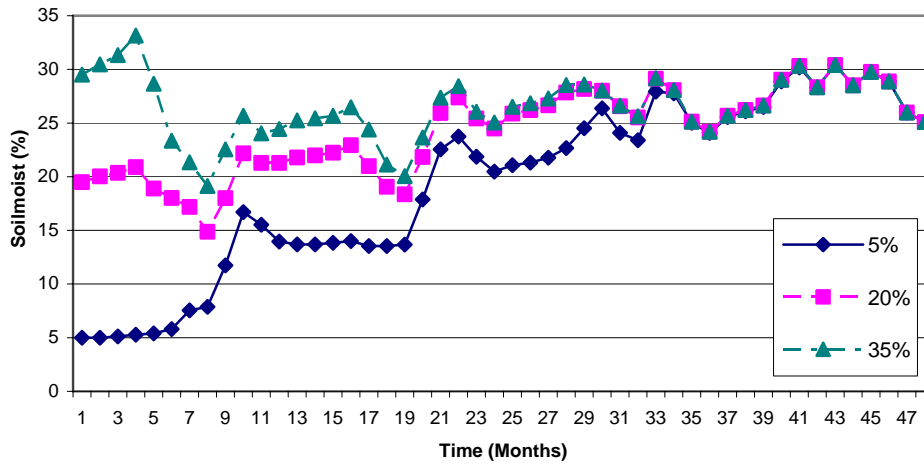


Figure 25. Development of simulated soil moisture due to different initial values. Simulated by Noah Layer 3 (40-100 cm) at the wetter location.

Initial Soilmoist Scenarios
CLM Layer 4 (9-17 cm), Dry location

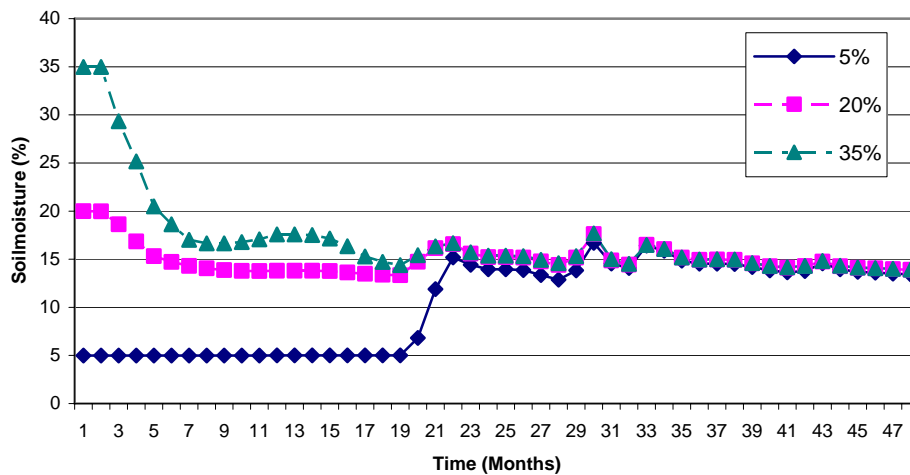


Figure 26. Development of simulated soil moisture due to different initial values. Simulated by CLM Layer 4 (9-17 cm) at the drier location.

8.2 Soil Moisture Simulation

8.2.1 Comparison of Noah and CLM Over a Four Year LIS run

All Noah and CLM soil moisture results can be viewed in Appendix V. Jiutaoli is presented below as Figure 27 because of its typical behaviour. By studying the graphs it looks like both models predicts similar trends. There are however some differences. Noah generally predicts more soil water than CLM does, especially during the winter months. From November to February there is usually an accumulation of water in the top layer in Noah and loss in CLM. The precipitation is very low for these months according to both models so this phenomenon is

quite strange. The soil moisture variable is defined as all available water, both liquid and frozen. It is possible that the divergence is caused by differences in the freezing processes, since this is the time of year when the region occasionally reaches subzero temperatures. A better understanding in the LSMs is however necessary to explain this. CLM does not seem to be finished with the spin up in the 40-100 and 100-200 cm layers after the four year simulation. There is an annual decrease in the CLM layers which can not be found in the Noah cases. The fluctuations are also generally higher for deeper layers in Noah.

There are many cases where the yearly fluctuations are higher in the Noah simulations, especially for the zone 3 locations. Among the studied zone 3 locations CLM shows less than 6 v% fluctuations for the whole period while Noah differ up to 15 v%.

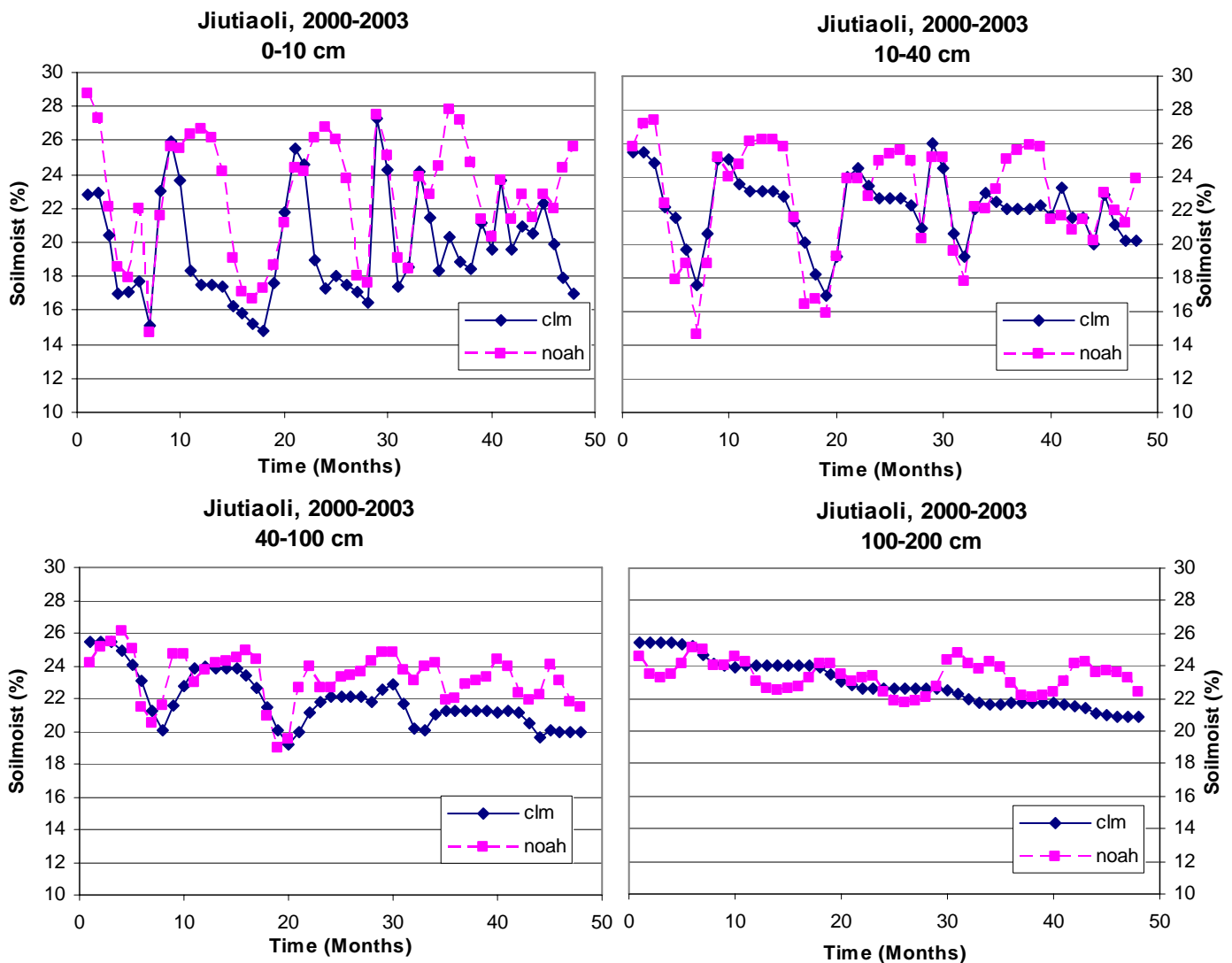


Figure 27. The simulated soil moisture for both models in the four layers at the Jiutiaoli point, presented as monthly averages.

The average four year soil moisture in the top layer is presented in Figure 28. Since the spin up time for this layer is only a few months for both models, the spin up effect is disregarded. Noah clearly shows higher levels of soil moist, often due to the difference during winter time. It is also clear that the soil is moister in height zone 1 than zone 2 and zone 2 is moister than zone 3, regardless of land use. The regional differences in soil moisture can also be viewed in Figure 29, showing the 2000-2004 average soil moisture for the CLM simulation.

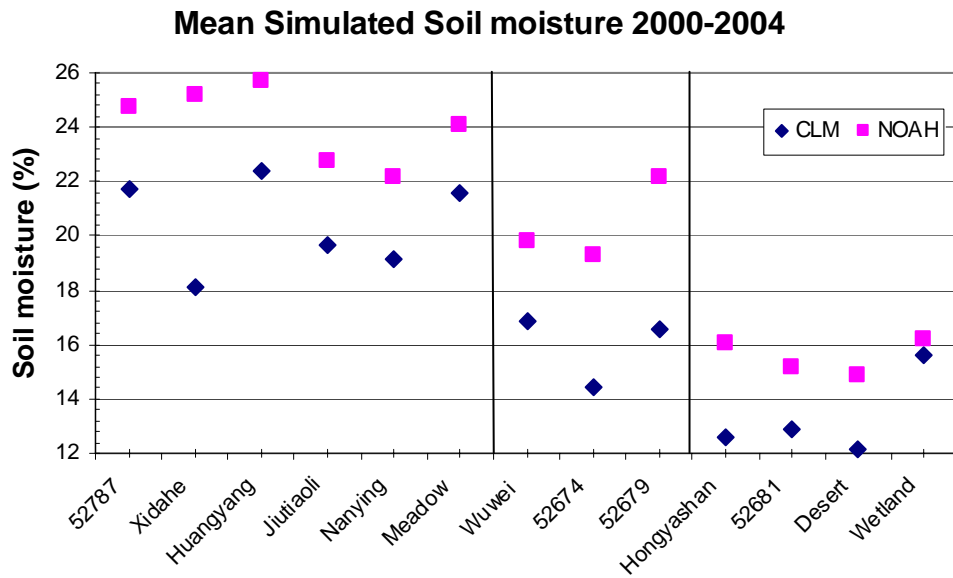


Figure 28. The mean soil moisture in the 0-10 cm layer over the four year simulation. The two lines separate the points into the three height zones. Zone 1, the wettest, is to the left, zone 2 in the middle and zone 3 to the right.

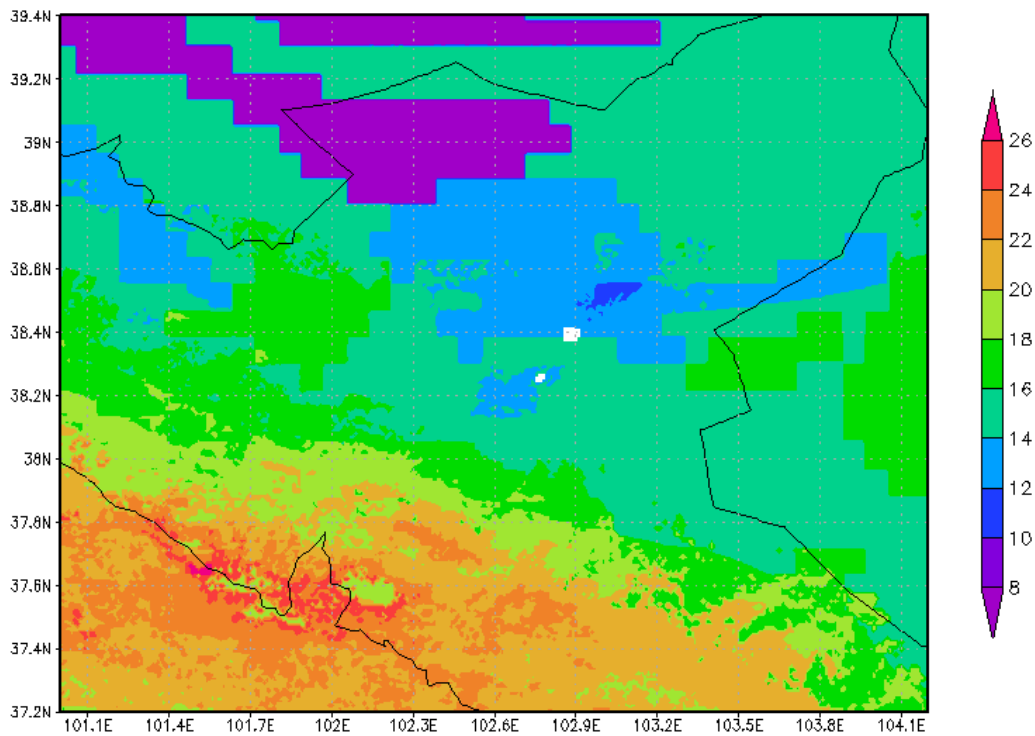


Figure 29. The average 2000-2004 soil moisture (%) from the CLM run.

An interesting observation was found when CLM was tested in combination with GEOS forcing. The initialization of the model resulted in absurd soil moisture results of about 6000% in the top layer. This problem was reported to the LIS support group at NASA and has been traced to the GEOS implementation of air temperature.

8.2.2 Modelling Constructed Rain

The infiltration pattern for the two LSMs could be viewed in Figure 30 and 31. The rain event caused a maximum increase in soil moisture of around 10 v% in the top 5 centimetres, and a maximum increase of about 5 v% at the depth of 20 cm for both LSMs. This occurred simultaneously for the two models after about 27 hours and 42 hours respectively. Percolated water seems unable to reach below the depth of 60 cm for CLM. Noah shows a water content increase of up to 2 v% at this depth after 72 hours. Notable is that percolated water even reach the depth of 150 cm in Noah.

After 168 hours soil water content is below initial values throughout the CLM profile with the exception of the depth 20-40 cm where one can see a minor increase. Noah on the other hand show soil moisture below initial values for the top layers but increasing moisture below the depth of 30 cm. Together with Noah's faster response in the top layers CLM appears to loose water while Noah show a higher storage capacity over time.

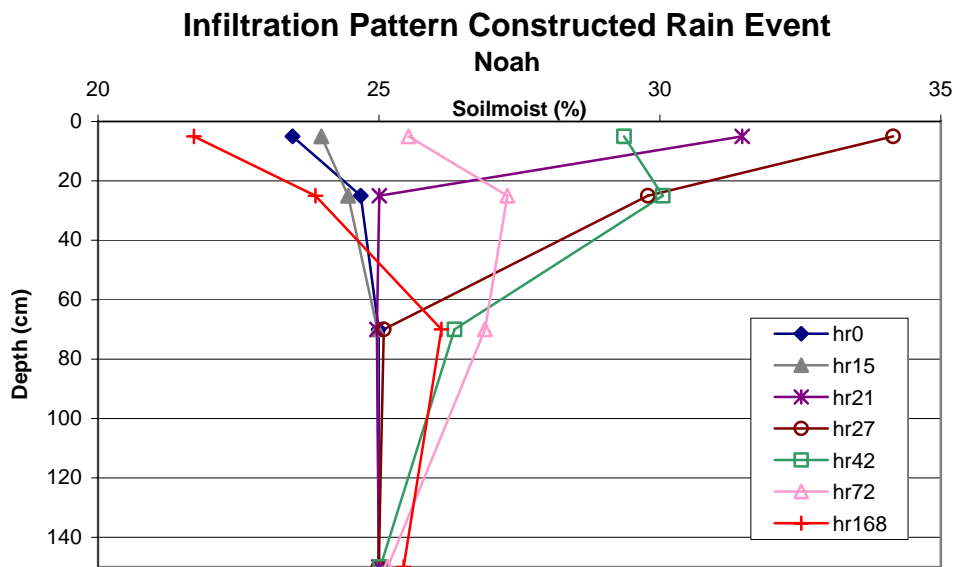


Figure 30. Soil moisture distribution along the soil profile for the constructed rain scenario. Water content is simulated with Noah and presented during the first 168 hours.

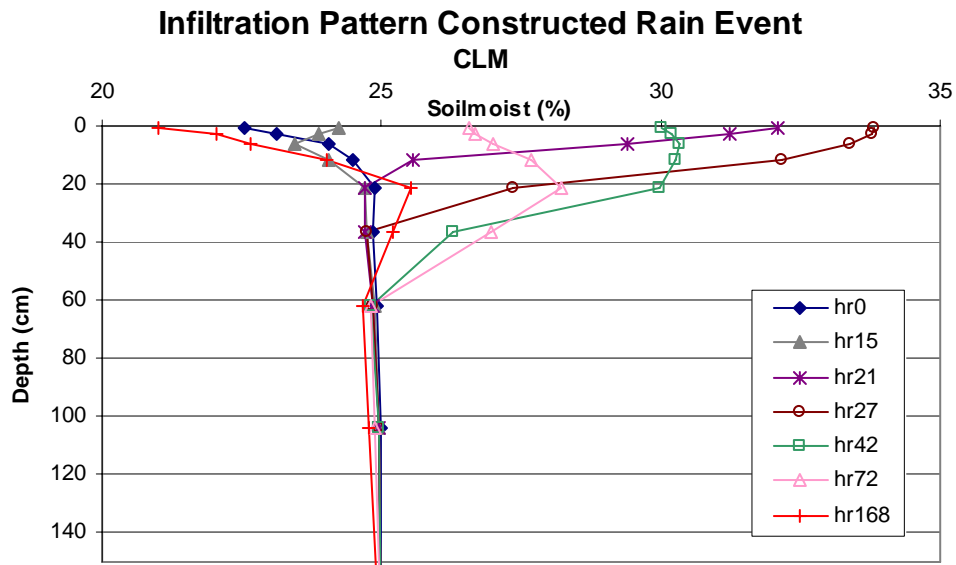


Figure 31. Soil moisture distribution along the soil profile for the constructed rain scenario. Water content is simulated with CLM and presented during the first 168 hours.

It seems like the infiltration process is quite similar in Noah and CLM in the upper layers but the water is unable to reach down to 60 centimetres in CLM, even after such intensive rainfall. The reason for this could be found by studying the other mechanisms; evaporation and surface and subsurface runoff. These can be studied in Figure 32 – 34. A simple water balance can be viewed in Table 9.

Table 9. A water balance for the constructed rain event for both model runs.

	Noah	CLM
Rainfall (mm)	34	34
Evaporation (mm)	28	22
Surface Runoff (mm)	1	12
Subsurface Runoff (mm)	4	9
Net (mm)	1	-9

The profile is almost unaffected by surface runoff in Noah while it contributes to an immediate loss of almost one third of the precipitated water in CLM. There is a surface runoff during the entire rain event in CLM, with a maximum rate of 1.2 mm/h at hour 27. The surface runoff in Noah also reached its maximum after 27 hours, corresponding to the CLM simulation but at a considerably lower rate of 0.1 mm/h

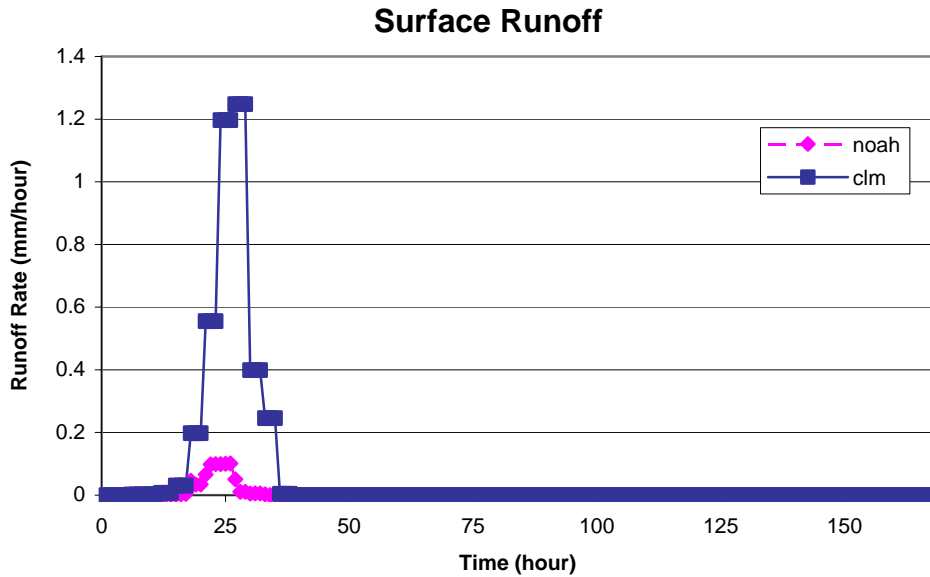


Figure 32. Surface runoff for both LSMs (Noah and CLM) during the constructed rain event.

Considering the subsurface runoff, CLM peaks after 75 hours and seems to drain the column to a larger extent than Noah. This could explain the quite rapid decrease in soil moisture at the depth of 40 cm occurring between hour 72 and 168 in the CLM profile. Since subsurface runoff affects layer 6 to 10 only, this would also be a possible reason for the water being unable to reach the 7th layer at 60 cm. The various flow rates could be due to the different interpretations of subsurface runoff. Since Noah and CLM have slightly different soil classifications, hydraulic properties could vary at the same location. This could influence water holding capacity and threshold levels dominating excess water and drainage.

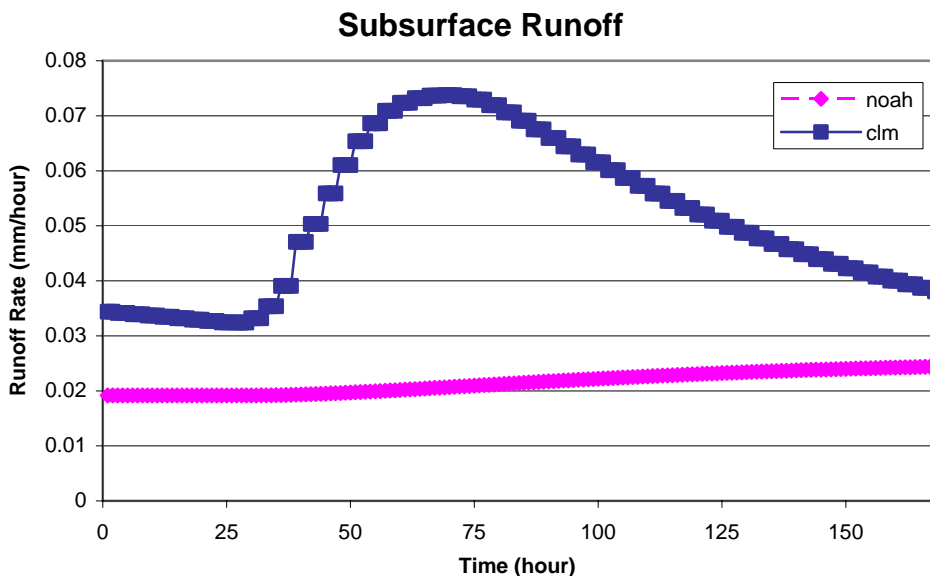


Figure 33. Subsurface runoff for both LSMs (Noah and CLM) during the constructed rain event.

Observing the evaporation, one can see that Noah tends to evaporate more than CLM. In the beginning CLM evaporates more than Noah, which changes just after the rain. Both models have corresponding diurnal manner with peaks during daytime. There appears to be a slight lag between the two, this could probably be explained with more frequent output of data. This causes Noah to respond to sudden small changes, which also explain the more oscillating behaviour during daytime.

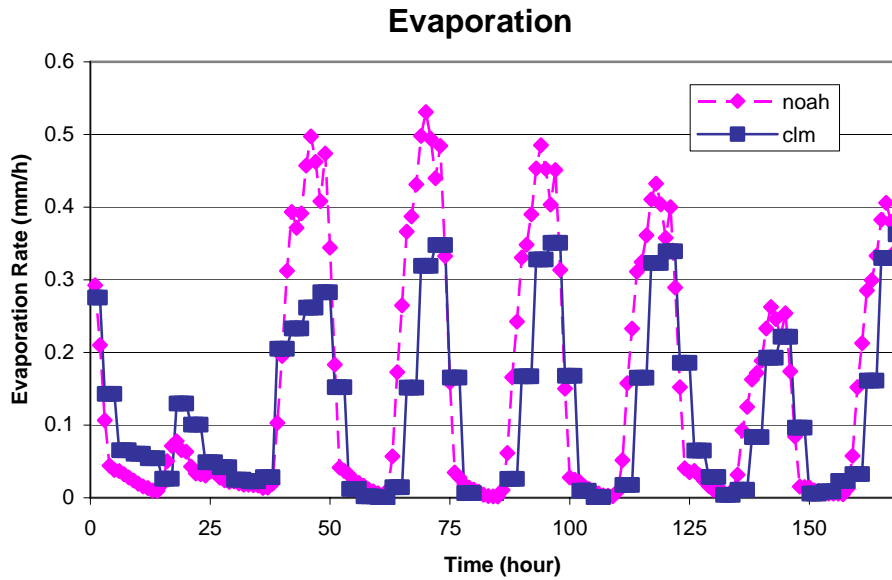


Figure 34. Evaporation for both LSMs (Noah and CLM) during the constructed rain event.

9 Conclusions

Simulating soil moisture accurately with large spatial cover and high resolution will be useful in combating desertification. LIS has the potential of being a tool for decision making, but is currently at a developing stage. We were able to find some problems and unresolved issues in the software. There are still tests and changes needed before it might be used in practice. At present a pre-release of LIS, version 5.0, is available indicating a constant research towards a more complete framework for land surface modelling.

We were unfortunately unable to use the results from the soil moisture experiments conducted in Wuwei in our study of LIS due to problems with the data server at NASA. As long as access to input data cannot be assured, the usefulness of LIS is very limited.

According to the set up test GDAS gave the best performance with LIS in terms of precipitation interpolation accuracy. Usage of supplementary forcing CMAP did not improve performance.

A slightly higher initial soil moisture than what is expected in a dry area could give shorter spin up time. This is probably due to high evaporation and lack of precipitation dominating the area. Reducing existing soil moisture requires a shorter time than accumulation to an accurate rate. Determination of an initial soil moisture state into one single mean value is however problematic and this is more evident for shorter simulations.

The four-year simulation indicated some differences between Noah and CLM. Noah seems to spin up faster than CLM, in all layers. The top layer of Noah tends to increase in soil moisture during winter, when CLM decreases. This is consistent for all locations and causes higher average soil water content for Noah.

In the constructed rain scenario water seems to percolate deeper and to a larger extent in Noah than in CLM. Noah accumulated water while CLM lost water. The reason could be traced to surface and subsurface runoff, where flow rates in CLM exceeded Noah's. In an arid area precipitated water is generally lost to evaporation rather than run off. This would normally indicate that Noah has a more accurate conceptual understanding of the infiltration processes. This precipitation scenario is however quite extreme and a deeper study of evaporation and run off in both models would be necessary to ensure which model is better.

Since validation data is missing, not much could be said about LSM reliability. Notable is that simulated values for the Wuwei area all exceed the measured values of September 2006. More and deeper studies of soil moisture fluctuations over time in these regions would be needed before anything can be said about the performance of the LSMs. Studies of actual and simulated surface and subsurface runoff could also give an indication of what LSM is more preferable in the region.

Despite its complexity, LIS is flexible and easy to use when set up correctly. There are however some difficult parts during compilation and set up and there is yet no proper manual.

References

Literature:

Box, George E. P., William G. Hunter, and J. Stuart Hunter, 1978. *Statistics for Experimenters, An Introduction to Design, Data Analysis, and Model Building*; John Wiley & Sons, Inc., ISBN 0-471-09315-7.

Ellis, S., and Mellor, A., 1995. *Soils and environment*. Routledge, New York. ISBN 0-415-06887-8

GPDPC and GPDWR (Gansu Provincial Development Planning Commission and Gansu Provincial Department of Water Resources), 2003. *The report on Programming for Comprehensive Rehabilitation of the Ecological Environment in the Shiyang River Basin*.

Runnström, M., 2003. *Land Degradation and Mitigation in northern China- Evaluated from the biological production*, Department of Physical Geography and Ecosystem Analysis, Lund University.

Soilmoisture equipment corp., 1996. *Trace operating instructions*.

Articles:

Chen, F., K. Mitchell, J. Schaake, Y. Xue, H.-L Pan, V. Koren, Q. Y. Duan, M. Ek and A. Betts, 1996. *Modelling of land surface evaporation by four schemes and comparison with FIFE observations*, Journal of Geophysical Research, Vol. 101, No. D3, p. 7251-7268, March 20.

Chen, F., Z. Janjic and K. Mitchell, 1997. *Impact of the atmospheric surface-layer parameterizations in the new land-surface scheme of NCEP mesoscale Eta model*, Boundary-Layer Meteorology 85: 391-421.

Chen, Y., and H. Tang, 2005. *Desertification in North China: Background, Anthropogenic Impacts and Failures in Combating it*, Land Degrad. Develop. 16:367-376

Dai, Y., X. Zheng, R. E. Dickinson, I. Baker, G. B. Bonan, M.G. Bosilovich, A. S. Denning, P. A. Dirmeyer, P. R. Houser, G. Niu, K. W. Oleson, C. A. Schlosser and Z.-L. Yang, 2003. *The Common Land Model*, American Meteorological Society, August.

Dirmeyer, P. A., Dolman, A. J., and Sato, N., 1999. *The Pilot Phase of the Global Soil Wetness Project*. Bulletin of the American Meteorological Society, vol. 80, Issue 5, pp.851-878

Ek, M. B., K. E. Mitchell, Y. Lin, E. Rogers, P. Grunmann, V. Koren, G. Gayno and J. D. Tarpley, 2003. *Implementation of Noah land surface model advances in the national Centers for Environmental Prediction operational mesoscale Eta model*, Journal of Geophysical Research, Vol. 108, No. D22, 8851, doi:10.1029/2002JD003296

Guo, Z. and Liu, H., 2005. *Eco-depth of groundwater table for natural vegetation in inland basin, northwestern China*. Journal of Arid Land Resources and Environment, 19(3), 157-161. (In Chinese)

Hu, Wenjun, 2005. *Water Resources Utilization and the Ecological Environment Protection in the Arid Inland Shiyang River Basin, Northwest China*. Proc. of Int. Symp. On Sustainable Water Res. Management and Oasis-hydrosphere-desert Interaction, 27-29, Oct., 2005.

Kang, S., X. Su, L. Tong, P. Shi, X. Yang, Y. Abe, T. Du, Q. Shen and J. Zhang, 2004. *The impacts of human activities on the water-land environment of the Shiyang River basin, an arid region in northwest China*, Hydrological Sciences-Journal des Sciences Hydrologiques, 49(3) June

Liao, L., Zhang, L., and Bengtsson, L. 2005. *Analysing Dynamic Change Of Vegetation Cover of Desert Oasis Based on remote Sensing Data in Hexi region*. Proc. of Int. Symp. On Sustainable Water Res. Management and Oasis-hydrosphere-desert Interaction, 27-29, Oct., 2005.

Liu, A.X., Liu Z. J., C. Y. Wang, and Z. Niu, 2003. *Monitoring of desertification in central Asia and western China using long term NOAA-AVHRR NDVI time-series data*. Geoscience and Remote Sensing Symposium, 2003. IGARSS apos;03. Proceedings. 2003 IEEE International Volume 4, Issue , 21-25 July 2003 Page(s): 2278 - 2280 vol.4

Oelert, A., and D. Rosbjerg, 2006. *Hydrological modelling of the surface water in the Shule River Basin*, Proc. Int. Symp. Sustainable Water Resources Management and Oasis-hydrosphere-desert Interaction in Arid Regions, 27-29 Oct., 2005, Beijing, p. 85-96.

Prince, S.D., 2002. *Spatial and Temporal Scales for Detection of Desertification*. *Global Desertification – do humans cause deserts?*, Ed. J.F. Reynolds and D.M. Stafford Smith. Dahlem University Press: 23-41.

Si, J., Gong, J., and Zhang, B., 2004. *The primary estimation of water demand for the eco-environment in arid regions*. Journal of Arid Land Resources and Environment, 18(1), 49-53 (In Chinese)

Yang, H., 2004. *Land conservation campaign in China: integrated management, local participation and food supply option*, Geoforum 35, p. 507-518

Yang, Y., Li, J., Chen, F., Burgess, J., Li, R., Li, D., Chang, G. and Li, Y., 2002. *The human mechanism research of Minqin Oasis change in the lower reaches of the Shiyang River*. Geography Research, 21(4), 449-458 (In Chinese)

Zhang, Y., 2001. *Minqin Oasis eco-environment degradation and rehabilitation approaches*. Design of Hydropower Stations, 17(4), 14-17. (In Chinese)

Zhao, X., 2005. *Study on the optimization and adjustment of agriculture industry structure to the water resource in Hexi Corridor of Gansu*. Journal of Arid Resources and Environment, 19(4), 7-12. (In Chinese)

Zhu, F., 2004. *Discussion on water resources development and comprehensive harnessing measures for eco-environment in Shiyang river basin*. Journal of Arid Land Resources & Water Engineering, 15(3), 45-48.
(In Chinese)

Internet:

CCICCD, 2006. *China National Report on the Implementation of the United Nation's Convention to Combat Deertification*. [online]

Available at:

<http://www.unccd.int/cop/reports/asia/national/2006/china-eng.pdf>, (2007-11-19)

LUNARC, 2007. *Systems* [online]

Available at:

<http://www.lunarc.lu.se/Systems> (2007-11-19)

NASA/GIOVANNI, 2007. *Daily Global and Regional Rainfall* [online]

Available at:

http://disc2.nascom.nasa.gov/Giovanni/tovas/realtime.3B42RT_daily.shtml 2007-11-19

NASA/GSFC, 2004. *Software Design Document for the Land Information System* [online]

Available at:

<http://lis.gsfc.nasa.gov/Overview/index.shtml> (2007-11-19)

NASA/GSFC, 2007. *Goddard Space Flight Center, Land Information System* [online]

Available at:

<http://lis.gsfc.nasa.gov/> (2007-11-19)

NASA/GSFC, 2007a. *Atmospheric Forcing Sample Data Documentation* [online]

Available at:

<http://lis.gsfc.nasa.gov/Data/LIS4.0/4.0.forcing.shtml>, (2007-11-19)

NRCS, 2007. *U.S. General Soil Map (STATSGO)* [online]

Available at:

<http://www.ncgc.nrcs.usda.gov/products/datasets/statsgo/> (2007-11-19)

NCAR, 2007. *Community Land Model* [online]

Available at:

<http://www.cgd.ucar.edu/tss/clm/> (2007-11-19)

NCEP, 2007. *Dataset (Global Tropospheric Analyses, 1999Sep-Present)* [online]

Available at:

<http://dss.ucar.edu/datasets/ds083.2/> (2007-11-19)

Mitchell K., 2001. *The community NOAA land-surface model (LSM)*

Available at:

http://www.emc.ncep.noaa.gov/mmb/gcp/noahls/README_2.2.htm (2007-11-19)

NOAA, 2002. *CPC Merged Analysis of Precipitation* [online]

Available at:

http://www.cpc.ncep.noaa.gov/products/global_precip/html/wpage.cmap.html, (2007-11-19)

NOAA, 2004. *Global Data Assimilation System (GDAS1) Archive Information* [online]

Available at:

<http://www.arl.noaa.gov/ss/transport/gdas1.html>, (2007-11-19)

NOAA, 2007. *Estimated Available Water Content from the FAO Soil Map of the World, Global Soil Profile Databases, and Pedo-transfer Functions* [online]

Available at:

<http://www.ngdc.noaa.gov/seg/cdroms/reynolds/reynolds/reynolds.htm>, (2007-11-19)

Oleson, K. W., Y. Dai et al., 2004. *Technical Description of the Community Land Model (CLM)* [online]

Available at:

<http://www.cgd.ucar.edu/tss/clm/distribution/clm3.0/index.html> (2007-11-19)

UMD, 2006. *UMD 1 km Global Land Coverage* [online]

Available at:

<http://www.geog.umd.edu/landcover/1km-map.html> (2007-09-11)

Vertenstein, M., K. Oleson, S. Levis and F. Hoffman, 2004. *Community Land Model Version 3.0 (CLM3.0) User's Guide, NCEP* [online]

Available at:

<http://www.cgd.ucar.edu/tss/clm/distribution/clm3.0/index.html> (2007-11-19)

World Climate, 2005. *World Climate* [online]

Available at:

<http://www.worldclimate.com> (2007-11-19)

Software and Datasets:

NCEP

Dataset (Global Tropospheric Analyses, 1999Sep-Present)

Available at:

<http://dss.ucar.edu/datasets/ds083.2/> (2007-11-19)

GrADS

Software

Institute of Global Environment and Society (IGES)

Available at:

<http://www.iges.org/> (2007-11-19)

LIS

Datasets and Software

Goddard Space Flight Center, NASA

Available at:

<http://lis.gsfc.nasa.gov/> (2007-11-19)

Appendices

Appendix A - Abbreviations

CAU	China Agricultural University
CCSM	Community Climate System Model
CGD	Climate and Global dynamics Division
CLM	Community Land Model
CMAP	CPC's Merged Analysis of Precipitation
CPC	Climate Prediction Center
DODS	Distributed Oceanographic Data System
E	Total Error
FAO	Food and Agriculture Organization
GDAS	Global Data Assimilation System
GDS	GrADS-DODS Server
GEOS	Goddard Earth Observing System
GIS	Geographic Information System
GPS	Global Position System
GrADS	Grid Analysis and Display System
GS-CIET	Gansu irrigation and training centre
GSFC	NASA Goddard Space Flight Centre
IGES	Institute for Global Environment and Society
LAI	Leaf Area Index
LIS	Land Information System
LSM	Land Surface Model
MAE	Mean Absolute Error
NASA	National Aeronautics and Space Administration
NCAR	National Centre for Atmospheric Research
NCEP	National Centre for Environmental Prediction
NDVI	Normalized Difference Vegetation Index
NOAA	National Oceanic Atmospheric Administration
NOAH	NCEP Oregon State University (Dept of Atmospheric Sciences) Air Force Weather Agency and Air Force Research Laboratory Hydrologic Research Lab
R	Sample correlation coefficient
SAI	Stem Area Index
SMW	Soil Map of the World
STATSGO	State Soil Geographic
TDR	Time Domain Reflectometry
UMD	University of Maryland

Appendix B - Precipitation Data

Hydrological Bureau of Gansu

Year	Month	Huangyang 黄羊河水库	Jiutiaoling 九条岭	Nanying 南营水库	Hongyashan 红崖山水库	Xidahe 西大河水库
2000	1	2,9	1,2	2,2	3,4	3,5
	2	5,2	2,5	2	3,1	7,1
	3	2,5	1,6	3,5	0	0,2
	4	20,3	8,2	12,5	8,9	13,7
	5	11,3	21,4	11,4	4,2	22,9
	6	67,7	107	88	51,2	110,8
	7	11	34,4	22,2	8,6	51,1
	8	71,4	70,8	66,2	25,6	84,9
	9	55,9	58,8	35,8	29,5	73,7
	10	14,9	5,3	11,8	10	16,5
	11	2,9	0,8	4,5	3,7	6,5
	12	0,9	1,8	0,8	0	0,7
2001	1	1,1	0,9	1,4	0	0,3
	2	0,5	1,3	0	0	0,7
	3	0	0,2	0	0	0,7
	4	21,9	13,3	13,4	2,2	13,3
	5	12	26,2	19,8	9,9	25,6
	6	8,8	21,9	8,4	0,8	37,3
	7	54,8	58,3	25,9	15,5	88,8
	8	71,1	62,8	50,1	19,1	55
	9	93,3	72,8	85,1	64,8	100,8
	10	21,8	14,4	18	9,4	13,4
	11	1,2	0,8	2,5	4,8	4,8
	12	1,1	3,5	2,5	2,4	2,4

Precipitation data China west

Year	Month	52674	52679	52681	52787
2001	1	0.5	0.3	0	3.5
	2	0	0	0	4.8
	3	0	0	0	1
	4	7.1	3.7	4.5	10.8
	5	15.9	18.5	13	37.7
	6	7.6	0.7	0.4	35.4
	7	41.9	22	11	111.6
	8	31.8	33.6	10.9	82.1
	9	65.1	63.1	41.6	78.2
	10	20.9	23.8	9.7	29.4
	11	2.4	2.4	4.2	0.3
	12	2.7	2.4	1.6	0.5
2002	1	2.6	4.1	1.1	4.7
	2	0	0	0	3.3
	3	0	4.4	0	5
	4	9.8	10.1	6	10.1
	5	58	47.5	40.9	81.3
	6	50.4	53.3	43.7	77.5
	7	43.2	12.8	19.6	29.2
	8	42.8	42.5	11.9	45.6
	9	56.1	59.6	30.9	72.4
	10	6.3	2.1	0.4	20.7
	11	1.6	5.9	0.1	5.8
	12	2.2	5.1	1.8	2.3
2003	1	1.2	3.2	1.3	0.3
	2	1.9	1.8	1.9	4.6
	3	8.7	4.8	4.5	10.4
	4	8.2	8.1	13.7	30.3
	5	32.6	29.6	11.6	69.9
	6	20.8	14.2	37.7	94
	7	29.6	24.4	21.3	94.7
	8	41.5	54.7	31.6	158.7
	9	29.7	16	12.2	44.2
	10	12.2	10.3	10.1	28.8
	11	5.8	7.9	3.1	7.3
	12	0.1	0.1	0	0.8

Appendix C - Soil Moist Measurements, Wuwei September 2006

Date	Type of equipment	Point nr	1		2		3		4		5		6		7	
	TDR	Soil moisture (v%)	0-10 cm	0-30 cm	0-10 cm	0-30 cm	0-10 cm	0-30 cm	0-10 cm	0-30 cm	0-10 cm	0-30 cm	0-10 cm	0-30 cm	0-10 cm	0-30 cm
09/05/2006									6.8	6	21.2	29.6				
09/06/2006			9.5	20.3	7.9	8.4	10.4	14.5	6.5	6	23.4	29.2	6.3	6.9	5.7	4.8
09/07/2006			9.6	16.5	7.5	7.8	10.7	16.9	6.1	5.6	23.4	33.6	5.2	4.5	5.4	4.8
	PVC	Soil moisture (v%)	0-10 cm	10-30 cm	0-10 cm	10-30 cm	0-10 cm	10-30 cm	0-10 cm	10-30 cm	0-10 cm	10-30 cm	0-10 cm	10-30 cm	0-10 cm	10-30 cm
09/13/2006				24.1	8.1	5			4.2	4.3	8.6	28	5.2	2.8	4.1	2.4
09/14/2006			2.6	24	3.7	4.7	2.5	13.9	3.4	3.9	22.9	29.7				
09/15/2006													1.3	1.8	1.8	1.7
	Drill															
09/13/2006			9.1				9.2									
09/16/2006			5.8	24.4	3.4	5.1	2.1	22.8								
09/17/2006					3.1	4.8			2.5	4	9.1	32.6	1.4	3.1	1.6	2.5
09/21/2006											22.4	36.4	0.8	2.2	0.3	1.6
09/22/2006			11.4	25.9	1.8	4.8	1.3	13.6	1.2	3.4						
09/23/2006																1.6
09/24/2006			9.5	26.6	6.2	4.6	5.4	19.1	4.8	3.2	16.9	26.6		1.4		
09/26/2006			7.5	20	4.6	5.4	9.4	23.5	4.3	3.7	22.4	22.1	5.4	2	5.3	2
09/27/2006			8.9	31.8	4.7	4.7	4.6	15.1	4.2	3.2	14.1	21.8	3.5	1.7	4.4	
09/28/2006			11.8	33.6	5	4.6	10.9	25.6	4.6	4.2	27.5	34.3	4.5	2.8	3.7	1.9

Date	Type of equipment	Point nr	8		9		10		11		12		13	
	TDR	Soil moisture (v%)	0-10 cm	0-30 cm	0-10 cm	0-30 cm	0-10 cm	0-30 cm	0-10 cm	0-30 cm	0-10 cm	0-30 cm	0-10 cm	0-30 cm
09/05/2006														
09/06/2006			7.4	5.9	5.9	5.6	18.3	21.9	6.1	4.9	5.8	5.4	5.8	5.3
09/07/2006			7.4	5.4	6.3	5.9	17	23.2	5.5	4.8	5.9	5.4	6.1	5.6
	PVC	Soil moisture (v%)	0-10 cm	10-30 cm	0-10 cm	10-30 cm	0-10 cm	10-30 cm	0-10 cm	10-30 cm	0-10 cm	10-30 cm	0-10 cm	10-30 cm
09/13/2006														
09/14/2006														
09/15/2006			3.4	2.7	2.7	2.7	20.7	21	2.2	1.9	2.8	3.9	2.7	2.6
	Drill													
09/13/2006														
09/16/2006														
09/17/2006			4.2	2.9	2.3	3.1								
09/21/2006														
09/22/2006							18.8	27.3	0.6	1.7	1.3	2.8	0.9	2
09/23/2006			1	2.7	0.8	3.2	26.8	25.9	3.2	3.3	0.9	2	0.6	2.2

Appendix D – File Examples

Statistical summary

Statistical Summary of Noah output for: 6/ 1/2002 0: 0: 0

	Mean	Stdev	Min	Max
Rainf(kg/m2s)	0.000E+00	0.000E+00	0.000E+00	0.000E+00
Evap(kg/m2s)	0.201E-04	0.142E-05	0.174E-04	0.237E-04
SoilMoist(kg/m2)	0.100E+02	0.526E-03	0.100E+02	0.100E+02
SoilMoist(kg/m2)	0.300E+02	0.469E-03	0.300E+02	0.300E+02
SoilMoist(kg/m2)	0.600E+02	0.303E-03	0.600E+02	0.600E+02
SoilMoist(kg/m2)	0.100E+03	0.000E+00	0.100E+03	0.100E+03

Statistical Summary of Noah output for: 6/ 1/2002 1: 0: 0

	Mean	Stdev	Min	Max
Rainf(kg/m2s)	0.000E+00	0.000E+00	0.000E+00	0.000E+00
Evap(kg/m2s)	0.409E-04	0.312E-05	0.342E-04	0.470E-04
SoilMoist(kg/m2)	0.999E+01	0.276E-02	0.999E+01	0.100E+02
SoilMoist(kg/m2)	0.300E+02	0.230E-02	0.300E+02	0.300E+02
SoilMoist(kg/m2)	0.600E+02	0.118E-02	0.600E+02	0.600E+02
SoilMoist(kg/m2)	0.100E+03	0.000E+00	0.100E+03	0.100E+03

Statistical Summary of Noah output for: 6/ 1/2002 2: 0: 0

	Mean	Stdev	Min	Max
Rainf(kg/m2s)	0.000E+00	0.000E+00	0.000E+00	0.000E+00
Evap(kg/m2s)	0.450E-04	0.268E-05	0.395E-04	0.508E-04
SoilMoist(kg/m2)	0.998E+01	0.599E-02	0.997E+01	0.999E+01
SoilMoist(kg/m2)	0.300E+02	0.721E-02	0.300E+02	0.300E+02
SoilMoist(kg/m2)	0.600E+02	0.343E-02	0.600E+02	0.600E+02
SoilMoist(kg/m2)	0.100E+03	0.000E+00	0.100E+03	0.100E+03

Statistical Summary of Noah output for: 6/ 1/2002 3: 0: 0

	Mean	Stdev	Min	Max
Rainf(kg/m2s)	0.000E+00	0.000E+00	0.000E+00	0.000E+00
Evap(kg/m2s)	0.378E-04	0.399E-05	0.291E-04	0.427E-04
SoilMoist(kg/m2)	0.996E+01	0.108E-01	0.994E+01	0.998E+01
SoilMoist(kg/m2)	0.300E+02	0.178E-01	0.299E+02	0.300E+02
SoilMoist(kg/m2)	0.600E+02	0.810E-02	0.600E+02	0.600E+02
SoilMoist(kg/m2)	0.100E+03	0.000E+00	0.100E+03	0.100E+03

Statistical Summary of Noah output for: 6/ 1/2002 4: 0: 0

	Mean	Stdev	Min	Max
Rainf(kg/m2s)	0.000E+00	0.000E+00	0.000E+00	0.000E+00
Evap(kg/m2s)	0.178E-04	0.408E-05	0.876E-05	0.234E-04
SoilMoist(kg/m2)	0.993E+01	0.168E-01	0.991E+01	0.998E+01
SoilMoist(kg/m2)	0.299E+02	0.325E-01	0.299E+02	0.300E+02
SoilMoist(kg/m2)	0.600E+02	0.150E-01	0.600E+02	0.600E+02
SoilMoist(kg/m2)	0.100E+03	0.000E+00	0.100E+03	0.100E+03

LIS config-file

```
#Overall driver options
Running mode:          1 # 1-retrospective , 2-AFWA AGRMET mode
Domain type:          1 # 1-latlon, 2-GSWP, 3-polar, 4-lambert
                        # 5-MERC, 6-AGRMET, 8-catchments
Number of subnests:   0 # 0 - 1 domain, 1 - one nest
Land surface model:   1 # 1-noah, 2-CLM, 3-VIC, 4-Hyssib,
                        # 7-Catchment
Base forcing source:   1 # 1-GDAS, 2-GEOS,3-ECMWF,
                        # 4-NLDAS,5-GSWP,6-BERG, 7-AGRMET
Supplemental forcing source: 0 # 0-none 2-CMAP

#The following options list the choice of parameter maps to be
#used
Landcover data source: 1 # 1-UMD, 2-USGS
Use soil texture:      0 # 1-use, 0-do not use
Soil data source:      1 # 1-FAO, 2-STATSGO
Soil color data source: 1 # 0-do not use, 1-FAO, 2-STATSGO
Topography data source: 1 # 0-do not use, 1-read LIS elevation file
LAI data source:       0 # 0-do not use, 1-AVHRR, 2-MODIS
Albedo data source:    1 # 0-do not use, 1-NCEP
Greenness data source: 1 # 0-do not use, 1-NCEP
Porosity data source:  0 # 0-do not use
Ksat data source:      0 # 0-do not use
B parameter data source: 0 # 0-do not use
Quartz data source:    0 # 0-do not use
Snow data source:      0 # 0-do not use

#Runtime options
Experiment code:       'exj' #max 3 character experiment code
Number of veg types:   13 #for UMD
Number of forcing variables: 10
Use elevation correction: 0 #0- do not use, 1-use lapse rate
Spatial interpolation method: 1 #1-bilinear, 2-conservative
Temporal interpolation method: 1 #1-linear,2-ubernext
Output forcing:        0 #0- no, 1-yes
Output methodology:    2 #0- no output,1-tiled, 2-gridded
Output data format:    1 #1-binary,2-grib,3-netcdf
Logging level:         1 #1-basic, 2-detailed, 3-debug
Start mode:            2 #1-restart,2-coldstart
Starting year:         2000
Starting month:        1
Starting day:          1
Starting hour:         0
Starting minute:       0
Starting second:       0
Ending year:          2004
Ending month:         1
Ending day:           1
Ending hour:          0
Ending minute:        0
Ending second:        0
Model timestep:       1800 #of the outer nest, in seconds
Undefined value:      -9999
Output directory:     '/disk/project1/zt/OUTPUT/' #what else is there?
Diagnostic output file: 'lisdiag'
Number of ensembles per grid: 1

#The following options are used for subgrid tiling based on vegetation
Maximum number of tiles per grid: 1
Cutoff percentage:    0.05

#Processor Layout
#Should match the total number of processors used

Number of processors along x: 2
Number of processors along y: 2

#Data Assimilation Options
Assimilation algorithm: 0 #0-none,1-direct insertion,
                        #2-EKF,3-EnKF
Variable being assimilated: 1 #1-Soil moisture
Observation data source: 0 #0-dummy data, 1-TMI
```

```

#Ensemble Propagation options

Ensemble propagation algorithm: 0 # 0-none, 1-Rolf's

#-----DOMAIN SPECIFICATION-----
#Definition of Running Domain
#Specify the domain extremes in latitude and longitude

run domain lower left lat:          37.155
run domain lower left lon:         100.995
run domain upper right lat:        39.445
run domain upper right lon:       104.195
run domain resolution dx:          0.01
run domain resolution dy:          0.01

#Definition of Parameter Domain

param domain lower left lat:       -59.995
param domain lower left lon:      -179.995
param domain upper right lat:      89.995
param domain upper right lon:     179.995
param domain resolution dx:        0.01
param domain resolution dy:        0.01

#-----PARAMETERS-----
#Metadata for Parameter maps
#Landcover and Landmask

landmask file:                     ./LIS_DATA/UMD_601KMmask.lgd4r
landcover file:                    ./LIS_DATA/UMD_601KM.lgd4r
landcover lower left lat:          -59.995
landcover lower left lon:          -179.995
landcover upper right lat:         89.995
landcover upper right lon:        179.995
landcover resolution (dx):         0.01
landcover resolution (dy):         0.01

#Topography maps
elevation map:                     ./LIS_DATA/lis_elev.lgd4r
slope map:
aspect map:
curvature map:
topography lower left lat:         -59.995
topography lower left lon:         -179.995
topography upper right lat:        89.995
topography upper right lon:        179.995
topography resolution (dx):        0.01
topography resolution (dy):        0.01

#Soils maps
#saturated matric potential - psisat
#saturated hydraulic conductivity - ksats
soil texture map:                  ./LIS_DATA/statsgo_tex.lgd4r
sand fraction map:                 ./LIS_DATA/sand60_1KM.lgd4r
clay fraction map:                 ./LIS_DATA/clay60_1KM.lgd4r
silt fraction map:                 ./LIS_DATA/silt60_1KM.lgd4r
soil color map:                   ./LIS_DATA/soicol_1KM.lgd4r
porosity layer1 map:
porosity layer2 map:
porosity layer3 map:
saturated matric potential map:
saturated hydraulic conductivity map:
b parameter map:                   ./gswp2data/Fixed/W_bpower_CEA84.nc
quartz map:
soils lower left lat:              -59.995
soils lower left lon:              -179.995
soils upper right lat:             89.995
soils upper right lon:             179.995
soils resolution (dx):             0.01
soils resolution (dy):             0.01

#Albedo maps
albedo map:                        ./LIS_DATA/alb
albedo climatology interval: 3 #in months

```

```

max snow free albedo map:    ./LIS_DATA/global_mxsnalb.1km.1gd4r
bottom temperature map:    ./LIS_DATA/tbot_1KM.1gd4r
greenness fraction map:    ./LIS_DATA/green
greenness climatology interval:    1    #in months

#LAI maps
LAI map:                    ./LIS_LAI/AVHRR_LAI_CLIM
SAI map:                    ./LIS_LAI/AVHRR_SAI_CLIM

#snow depth maps
Snow depth map:            ./FORCING/AFWA/

# Catchment based tile map
tile coord file:          ./cat_parms_new/PE_360x180_DE_288x270_DE.til
tile veg file:            ./cat_parms_new/mosaic_veg_typs_fracs
#-----FORCINGS-----
#GDAS (forcing option =1) forcing=15
GDAS forcing directory:   ./LIS_FC/GDAS
GDAS elevation map:      ./LIS_DATA/gdasnew_elev.1gd4r
GDAS elevation map change 1:  ./LIS_DATA/gdasnew_elev.1gd4r
GDAS elevation map change 2:  ./LIS_DATA/gdasnew_elev.1gd4r
GDAS elevation map change 3:  ./LIS_DATA/gdasnew_elev.1gd4r
GDAS domain x-dimension size: 512
GDAS domain y-dimension size: 256
GDAS number of forcing variables: 10

#GEOS (forcing option =2)
GEOS forcing directory:   ./LIS_FC/GEOS ""
GEOS domain x-dimension size: 360 360
GEOS domain y-dimension size: 181 181
GEOS number of forcing variables: 13 13

#CPC CMAP precipitation (observed forcing option = 2)
CMAP forcing directory:   ./LIS_FC/CMAP
CMAP domain x-dimension size: 512
CMAP domain y-dimension size: 256

#-----LAND SURFACE MODELS-----
#NCEP's NOAH (lsm option =1)
NOAH model output interval:    3600    #in seconds
NOAH restart output interval:  86400    #in seconds
NOAH restart file:            noah-rs
NOAH slope file:
NOAH vegetation parameter table:  ./LIS_BCS/noah_parms/noah.vegparms.txt
NOAH soil parameter table:      ./LIS_BCS/noah_parms/noah.soilparms.txt
NOAH general parameter table:   ""    ./LIS_BCS/noah_parms/GENPARM.UNIF.TBL
NOAH bottom temperature climatology interval: 0 # in months, 0-static
NOAH number of vegetation parameters: 7
NOAH soils scheme:            1    #1-zobler, 2-statsgo
NOAH number of soil classes:   9    #9 for zobler, 19 for statsgo, 16 afw
NOAH number of soil layers:    4
NOAH observation height:      10    #meters
NOAH initial soil moisture:    0.25 # % volumetric
NOAH initial soil temperature: 272.2 # Kelvin

#NCAR's CLM2.0 (lsm option =2)
CLM model output interval:    10800
CLM restart output interval:  86400
CLM restart file:            clm2.rst
CLM vegetation parameter table:  ./LIS_BCS/clm_parms/umdvegparam.txt
CLM canopy height table:      ./LIS_BCS/clm_parms/clm2_ptcanhts.txt
CLM initial soil moisture:    0.45 # % volumetric
CLM initial soil temperature:  290.0 # Kelvin
CLM initial snow mass:        0.0

#-----MODEL OUTPUT CONFIGURATION-----
#Specify the list of ALMA variables that need to be featured in the
#LSM model output

#Energy balance components
Swnet:    0    # Net Shortwave Radiation (W/m2)
Lwnet:    0    # Net Longwave Radiation (W/m2)
Qle:      0    # Latent Heat Flux (W/m2)
Qh:       0    # Sensible Heat Flux (W/m2)

```

```

Qg:          0      # Ground Heat Flux (W/m2)
Qf:          0      # Energy of fusion (W/m2)
Qv:          0      # Energy of sublimation (W/m2)
Qa:          0      # Advective Energy (W/m2)
Qtau:        0      # Momentum flux (N/m2)
DelSurfHeat: 0      # Change in surface heat storage (J/m2)
DelColdCont: 0     # Change in snow cold content (J/m2)

#Water balance components
Snowf:       0      # Snowfall rate (kg/m2s)
Rainf:       1      # Rainfall rate (kg/m2s)
Evap:        1      # Total Evapotranspiration (kg/m2s)
Qs:          0      # Surface runoff (kg/m2s)
Qrec:        0      # Recharge (kg/m2s)
Qsb:         0      # Subsurface runoff (kg/m2s)
Qsm:         0      # Snowmelt (kg/m2s)
Qfz:         0      # Refreezing of water in the snowpack (kg/m2s)
Qst:         0      # Snow throughfall (kg/m2s)
DelSoilMoist: 1     # Change in soil moisture (kg/m2)
DelSWE:      0      # Change in snow water equivalent (kg/m2)
DelSurfStor: 0     # Change in surface water storage (kg/m2)
DelIntercept: 0    # Change in interception storage (kg/m2)

#Surface State Variables
SnowT:       0      # Snow surface temperature (K)
VegT:        0      # Vegetation canopy temperature (K)
BareSoilT:   0      # Temperature of bare soil (K)
AvgSurfT:    0      # Average surface temperature (K)
RadT:        0      # Surface Radiative Temperature (K)
Albedo:      0      # Surface Albedo (-)
SWE:         0      # Snow Water Equivalent (kg/m2)
SWEVeg:      0      # SWE intercepted by vegetation (kg/m2)
SurfStor:    0      # Surface water storage (kg/m2)

#Subsurface State Variables
SoilMoist:   1      # Average layer soil moisture (kg/m2)
SoilTemp:    0      # Average layer soil temperature (K)
SmLiqFrac:   0      # Average layer fraction of liquid moisture (-)
SmFrozFrac:  0      # Average layer fraction of frozen moisture (-)
SoilWet:     0      # Total soil wetness (-)

#Evaporation components
PotEvap:     0      # Potential Evapotranspiration (kg/m2s)
ECanop:      0      # Interception evaporation (kg/m2s)
TVeg:        0      # Vegetation transpiration (kg/m2s)
ESoil:       0      # Bare soil evaporation (kg/m2s)
EWater:      0      # Open water evaporation (kg/m2s)
RootMoist:   0      # Root zone soil moisture (kg/m2)
CanopInt:    0      # Total canopy water storage (kg/m2)
EvapSnow:    0      # Snow evaporation (kg/m2s)
SubSnow:     0      # Snow sublimation (kg/m2s)
SubSurf:     0      # Sublimation of the snow free area (kg/m2s)
ACond:       0      # Aerodynamic conductance

```

Ctl-file

```
DSET ^NOAH/%y4/%y4%m2%d2/%y4%m2%d2%h2%n2.d01.gs4r
options template
options sequential
options big_endian
TITLE Noah ShangYeah 1Km 2001
UNDEF -9999.0
XDEF 321 LINEAR 101 0.01
YDEF 230 LINEAR 37.16 0.01
ZDEF 1 LINEAR 1 1
TDEF 35064 LINEAR 00Z01jan2000 1hr
VARS 6
Rainf 1 99 ** 1 Rainfall rate kg/m^2/s
Evap 1 99 ** 2 Total Evapotranspiration kg/m^2/s
SoilMoist1 1 99 ** 3 Average layer 1 soil moisture kg/m^2
SoilMoist2 1 99 ** 4 Average layer 2 soil moisture kg/m^2
SoilMoist3 1 99 ** 5 Average layer 3 soil moisture kg/m^2
SoilMoist4 1 99 ** 6 Average layer 4 soil moisture kg/m^2
ENDVARS
```


UMD Vegetation Classification

Class value and description

0	Water
1	Evergreen Needleleaf Forest
2	Evergreen Broadleaf Forest
3	Deciduous Needleleaf Forest
4	Deciduous Broadleaf Forest
5	Mixed Forest
6	Woodland
7	Wooded Grassland
8	Closed Shrubland
9	Open Shrubland
10	Grassland
11	Cropland
12	Bare Ground
13	Urban and Built-up

Appendix E - Comparison of Noah and CLM over a Four Year LIS Run

